BRIGHAM YOUNG UNIVERSITY

GEOLOGY

S T U D I E S

GEOLOGICAL SOCIETY OF AMERICA

FIELD TRIP GUIDE BOOK

1997 ANNUAL MEETING • SALT LAKE CITY, UTAH

PART 1 ONE

EDITED BY PAUL KARL LINK AND BART J. KOWALLIS

VOLUME 42 • 1997

Bimodal Magmatism, Basaltic Volcanic Styles, Tectonics, and Geomorphic Processes of the Eastern Snake River Plain, Idaho

SCOTT S. HUGHES
Department of Geology, Idaho State University, Pocatello, Idaho

RICHARD P. SMITH
Idaho National Engineering and Environmental Laboratory, Idaho Falls, Idaho

WILLIAM R. HACKETT
WRH Associates, Salt Lake City, Utah

MICHAEL McCURRY
Department of Geology, Idaho State University, Pocatello, Idaho

STEVEN R. ANDERSON
U.S. Geological Survey, Idaho Falls, Idaho

GREGORY C. FERDOCK
Mackay School of Mines, University of Nevada, Reno, Reno, Nevada

ABSTRACT

Geology presented in this field guide covers a wide spectrum of internal and surficial processes of the eastern Snake River Plain, one of the largest components of the combined late Cenozoic igneous provinces of the western United States. Focus is on widespread Quaternary basaltic plains volcanism that produced coalescent shields and complex eruptive centers that yielded compositionally evolved magmas. The guide is constructed in several parts beginning with discussion sections that provide an overview of the geology followed by road directions, with explanations, for specific locations. The geology overview briefly summarizes the collective knowledge gained, and petrologic implications made, over the past few decades. The field guide covers plains volcanism, lava flow emplacement, basaltic shield growth, phreatomagmatic eruptions, and complex and evolved eruptive centers. Locations and explanations are also provided for the hydrogeology, groundwater contamination, and environmental issues such as range fires and cataclysmic floods associated with the region.

INTRODUCTION

The eastern Snake River Plain (ESRP) is an east-northeast-trending 600-km long, 100-km wide topographic depression extending from Twin Falls to Ashton, Idaho. Corporate agriculture, especially potatoes, grains and sugar beets, is the dominant economy supported by a vast groundwater and surface water system. The Idaho National Engineering and Environmental Laboratory (INEEL), a U.S. Department of Energy nuclear facility, covers about 2,315 km^2 of the ESRP, and much of the remaining rangeland, including that which is covered by relatively fresh lava flows, is controlled by the U.S. Bureau of Land Management. The terrain is semiarid steppe developed on eolian and lacustrine soils that variably cover broad expanses of basaltic lava. The ESRP is bounded on the north and south by mountains and valleys associated with the Basin and Range province. These mountains trend perpendicular to the axis of the Snake River Plain.

Several major late Tertiary geologic events are important to the formation of the ESRP. These include: (1) time-transgressive Miocene-Pliocene rhyolitic volcanism associated with the track of the Yellowstone hotspot, (2) Miocene to Recent crustal extension which produced the Basin and Range province, (3) Quaternary outpourings of basaltic lavas and construction of coalescent shield volcanoes, and (4) Quaternary glaciation and associated eolian and fluvial sedimentation, as well as lakes and periodic catastrophic floods. Environmental issues on the ESRP include natural hazards related to these events, especially volcanism and earthquakes, plus the availability of clean groundwater. An almost yearly occurrence of range fires with concomitant dust storms constitutes an additional geomorphic factor.

This field trip covers selected aspects of these issues, and their associated surface and subsurface processes. Previous studies of ESRP basaltic magmatism and surficial processes have provided the geologic basis for this article (e.g. Stearns et al., 1938; Prinz, 1970; various chapters in Greeley and King, 1977; Greeley, 1982; Kuntz et al., 1982, 1986a, 1986b, 1992, 1994; Malde, 1991; Pierce and Morgan, 1992; and many others). Published ESRP field guides include those by Greeley and King which presented ESRP volcanism as a terrestrial planetary analogue; Hackett and Morgan (1988) which dealt with explosive volcanism and focused on emplacement of rhyolite ash-flow sequences; Kuntz (1989) which concentrated on Craters of the Moon; and Hackett and Smith (1992) which dealt mainly with geology of the INEEL and surroundings. General aspects of ESRP geology are presented here, emphasizing the emplacement of non-explosive basaltic dikes and lavas, their compositions, topographically-imposing rhyolitic domes, and phreatomagmatic basaltic eruptions that are directly related to proximity of magma to the Snake River. Readers should refer to the guides mentioned above for more in-depth treatment of their respective topics.

The field trip plan is constructed around logistics of travel throughout the ESRP, rather than topics, because the locations of various styles of volcanism are intermixed. We have attempted to limit the inevitable overlap with other field trip guides to features that would be important to first-time visitors as well as seasoned ESRP geologists.

GEOLOGIC SETTING

Quaternary volcanic landforms, i.e., basaltic lava flows, small shield volcanoes, and rhyolitic domes dominate the physiography of the ESRP (Figs. 1 and 2) and the upper 1–2 km of the crust. Rhyolite domes (Fig. 3) and compositionally complex eruptive centers are most concentrated along the northeast-trending axial volcanic zone (Stops 5–9) which constitutes the topographically high central axis of the ESRP (Hackett and Smith, 1992; Kuntz et al., 1992). Most basalts typically erupt from fissures located along, and subparallel to, NW-SE volcanic rift zones that parallel Basin and Range structures in southern Idaho. Miocene-Pliocene rhyolitic ash-flow tuffs lie beneath the basaltic cover and are exposed in ranges along the margins of the ESRP (Fig. 2). These older rhyolitic caldera eruptions are associated with time-transgressive volcanism from SW Idaho at ~14 Ma to Yellowstone National Park at 2-0.6 Ma (Pierce and Morgan, 1992). Other ESRP volcanic features include several complex Quaternary eruptive centers comprised of pyroclastic cones, dikes, and chemically evolved lavas.

Widespread basaltic volcanic activity occurred intermittently on the ESRP throughout Pleistocene and Holocene time. Thickness of most individual basalt flows in the upper part of the volcanic section ranges from about 5m to as much as 25m, and the flows extend up to 48 km. The lavas are predominantly olivine tholeiites emplaced as channel or tube-fed pahoehoe flows from fissures associated with small shield volcanoes. Many individual lava flow units contribute to the growth of each shield over a few months or years. Eight such basaltic volcanic fields have formed since 15 ka (Fig. 2). These include the Shoshone, Wapi, Craters of the Moon (Stop 10), Kings Bowl (Stop 12), North Robbers (Stop 9), South Robbers, Cerro Grande (Stop 7), and Hells Half Acre (Stops 2 and 4) lava fields that cover approximately 13 percent of the ESRP.

Kuntz et al., (1992) estimate a magma output rate of 3.3 km^3 per 1000 years for the entire ESRP during the past 15,000 years. Petrologic studies (Leeman, 1982b; Leeman et al., 1976) indicate that ESRP basaltic lavas range from primary olivine tholeiites to evolved and contaminated compositions. The most widely known compositionally evolved center is Craters of the Moon volcanic field, comprising several individual eruptive centers active from 15 to 2 ka.

Because basaltic shields are topographically elevated, they control the deposition of younger sediments and lavas (Hughes et al., 1997). Modern sediments are distributed on the ESRP largely in loess, lacustrine (playa-like "sinks") and fluvial depositional systems (e.g. Hackett and Smith, 1992; Kuntz et al., 1992, 1994; Geslin et al., 1997; Gianniny et al., 1997). Playa sediments are clay-rich silt and fine-sand mixtures of eolian and stream-born material. Fluvial sediments are mostly coarser sand, pebbles and cobbles derived from the Big Lost River, Little Lost River, and Birch Creek drainages north of the INEEL. Loess also covers most pre-Holocene surfaces and also occurs as layers between lava flow groups in the subsurface. These processes will be discussed at Stop 5 while standing on East Butte rhyolite dome.

BIMODAL VOLCANISM ON THE EASTERN SNAKE RIVER PLAIN

Scott Hughes, Idaho State University, Pocatello, ID

The Yellowstone Hotspot

Volcanism associated with the Snake River Plain in Idaho and adjacent areas of Nevada and the Yellowstone plateau

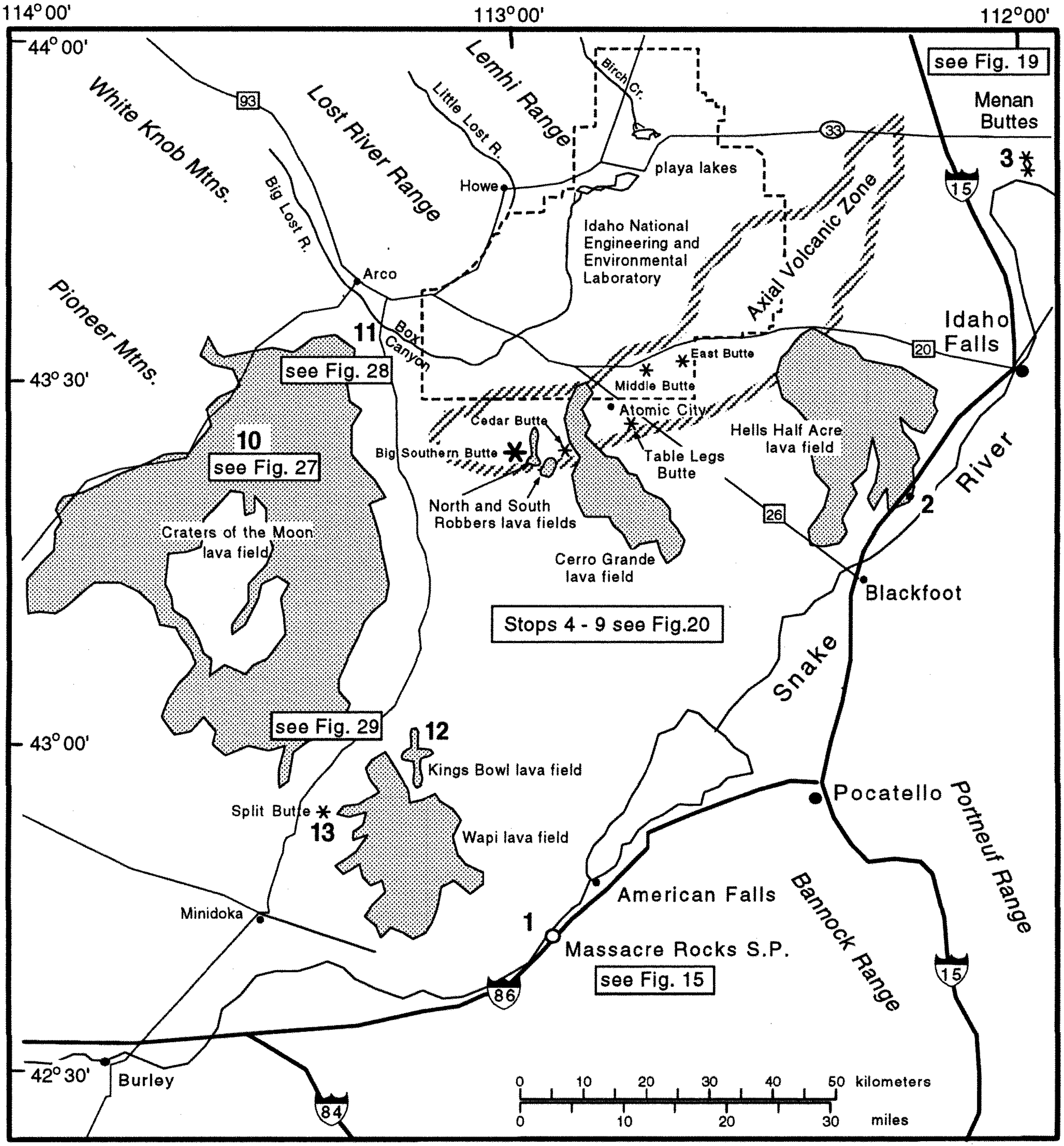

Figure 1. Map of the field trip area showing the location of the axial volcanic zone in relation to seven of eight latest Pleistocene-Holocene basaltic lava fields (shaded fields). Field trip stops, except stops 4–9 (see Fig. 20), are shown in boldface numbers. Refer to figure numbers in boxes for detailed road maps.

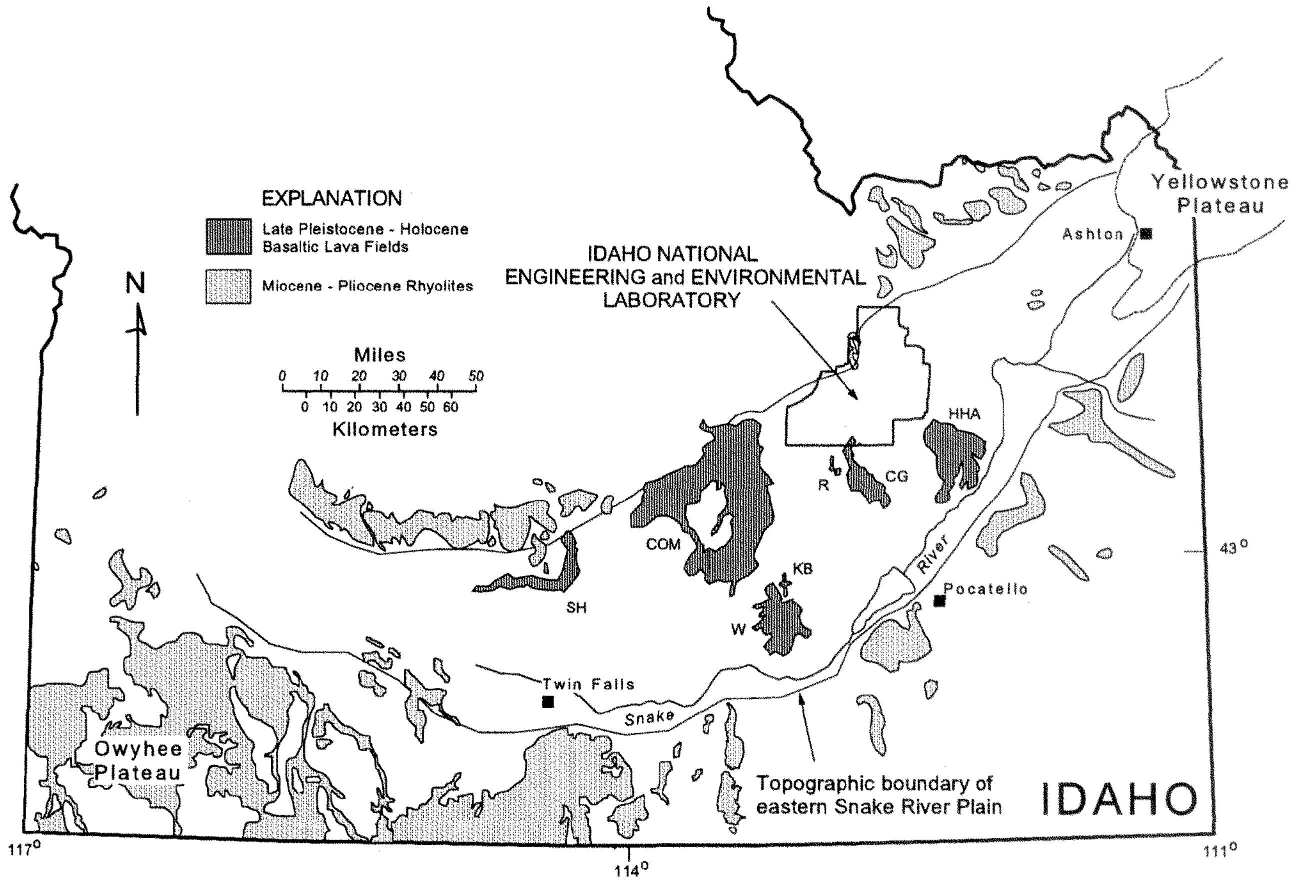

Figure 2. Map of southern Idaho and the eastern Snake River Plain showing locations of Owyhee Plateau, Yellowstone Plateau, Idaho National Engineering and Environmental Laboratory (INEEL), latest Pleistocene-Holocene basaltic fields (dark shading), and major outcrops of Miocene-Pliocene rhyolites. Abbreviations for lava fields are: SH = Shoshone, COM = Craters of the Moon, W = Wapi, KB = Kings Bowl, R = North and South Robbers, CG = Cerro Grande, and HHA = Hells Half Acre.

during the past 16 Ma is the manifestation of a bimodal (rhyolitic/basaltic) continental tectono-magmatic system. The Yellowstone-Snake River Plain (YSRP) volcanic system is largely made up of thick, time-transgressive rhyolitic ignimbrites and lavas caused by melting above a mantle hotspot (Pierce and Morgan, 1992; Smith and Braile, 1993). Age-progressive rhyolites are mainly exposed along the northern and southern boundaries of the ESRP, on the Yellowstone Plateau, and on the Owyhee Plateau of southwestern Idaho (Fig. 2).

Hypotheses invoked to explain this age progression, recognized by Armstrong et al., (1975) and reviewed by Pierce and Morgan (1992), include: (1) the trace of a stationary deep-seated mantle plume, currently beneath the northeast part of Yellowstone National Park (Morgan, 1972; Smith and Sbar, 1974); (2) an eastward propagating rift in the lithosphere, which caused melting of the asthenosphere by decompression (Myers and Hamilton, 1964; Hamilton, 1989); (3) volcanism along a preexisting crustal flaw (Eaton et al., 1975); (4) propagation of a crack following a transform fault boundary between two regimes of Basin and Range extension (Christiansen and McKee, 1978); and (5) a meteorite impact which initiated the eruption of large volumes of flood basalts (Alt et al., 1988). The most widely accepted of these five ideas is that the ESRP and its extensions was formed above a hotspot track, created by the passage of the North American plate southwestward over a stationary mantle plume (Armstrong et al., 1975; Leeman, 1982a; Pierce and Morgan, 1992; Smith and Braile, 1993). Late Tertiary tectonics in the northwestern U.S. yielded a complex magmatic system involving the Cascades, Columbia Plateau, Owyhee Plateau, Snake River Plain, and Yellowstone Plateau. Geist and Richards (1993) suggest that relative volcanic ages and positions of these regions can be explained by deflection of the rising mantle plume at ~20 Ma northward by the subducting Farallon plate. According to their model, the downgoing slab was subsequently penetrated at ~17.5 Ma and allowed the plume to pass through

Figure 3. View from East Butte looking west: Middle Butte (foreground, ~7 km distant) and Big Southern Butte (~30 km distant) rhyolitic domes on the Eastern Snake River Plain. Middle Butte is covered by Quaternary basalts that were uplifted during emplacement.

to produce the Columbia River Basalt and the Yellowstone hotspot track.

Estimated rates of southwestward movement of the North American continental plate range from 2.9–7 cm/yr, with an average rate of 4 ± 1 cm/yr (Smith and Braile, 1993). Pierce and Morgan (1992) indicate a shift in the hotspot track near Twin Falls that relates to decrease in rate of hotspot migration (7 cm/yr to 2.9 cm/yr) and change in direction (N70–75°E to N54°E). Accounting for Basin and Range extension along the hotspot track and Miocene-Pliocene plate rotation, Rodgers et al., (1990) determined a rate of 4.5 cm/yr and a direction of N56°E of the volcanic track over the last 16 Ma. Their model places the present position of the hotspot at least 90 km northeast of the oldest Yellowstone caldera.

Basaltic Plains Volcanism

Time-space relations of rhyolite and basalt are dissimilar. Although the inception of ESRP basaltic volcanism exhibits a general time-progressive trend (Armstrong et al., 1975), Pleistocene lavas occur over much of the ESRP. Up to 2 km of late Tertiary, Quaternary and Holocene diktytaxitic olivine tholeiite lavas covered the ESRP and lie above the Miocene-Pliocene rhyolites. Detailed surface maps by Kuntz (1979) and Kuntz et al., (1988, 1994), along with investigations into mechanisms of basaltic magmatism (Kuntz, 1992; Kuntz et al., 1982, 1986a, 1992) have lead to models of the magmatic sources and lithospheric plumbing systems. Fissure vents occur mainly along the NW-SE volcanic rifts zones.

Many of the ESRP volcanic landforms and eruptive mechanisms were described in Greeley and King (1977) and later in Greeley (1982), both of which developed the concept of basaltic "plains-style volcanism." Low-profile coalescent shields on the ESRP produce subdued topography and shallow depositional slopes. Most shields are formed by low-volume monogenetic eruptions over short time spans (Stops 2 and 4), so they have little opportunity for significant growth above the surrounding topographic surface. Interspersed among shields are complex volcanoes, largely associated with compositionally evolved lavas (Stop 8). They often include eruptive and non-eruptive fissures, evolved eruptive centers with composite cones, rhyolite domes, and sedimentary interbeds (Fig. 4).

Vent regions exhibit either spatter ramparts, which are positive topographic features, or broad collapse pits where lavas flowed through a breached portion of the shield. Lava flow sequences are readily observed in the walls of breached summits, such as at Black Butte Crater in the Shoshone lava field (Fig. 2) which produced an impressive 50-km-long tube-fed basaltic lava flow. Lava lakes form in vent areas also during the release of lava into tube-fed or channel-fed flow systems. Their presence is evident in young vents not obscured by loess (Fig. 5), such as the Pillar Butte eruptive center in the Wapi lava field (Fig. 2) which has a radiocarbon age of 2,270 ± 50 B.P. (Kuntz et al., 1986b). Lava lakes are evident in other vents although eolian deposits partially cover some of the late Pleistocene and Holocene systems.

Tectonic Influences on Basaltic Magmatism

Mechanisms of magma storage, dike injection and eruption, invoked from previous investigations and comparative detailed studies of other basaltic systems, allow some speculation of tectonic influences on ESRP magmatism. Volcanic rift zones on the ESRP are manifested by linear sequences of basaltic vents with associated fissure-fed flows and open fissures that are generally parallel to, but not collinear with, Basin and Range faults north and south of the plain (Kuntz et al., 1992). Surface deformation in areas near eruptive centers includes linear fractures, grabens and monoclines due to shallow magma injection (Stops 4 and 9–12). Orientation of inferred basaltic feeder dikes, as evidenced by the strong alignments of surface deformation features and vents, suggests that they reflect, at least in part, a regional SW-NE direction of extensional stress or of least-compressive stress.

Tectonic SW-NE extension on the ESRP is believed to be accommodated more by dike injection than faulting (Hackett and Smith, 1992), although in the Basin and Range province the lithosphere extends by normal faulting. Regional stress apparently affects basaltic magma emplacement in reservoirs in the upper mantle or lower crust where primary melts accumulate above the region of partial melting. The magmatic model by Kuntz (1992) suggests that basaltic

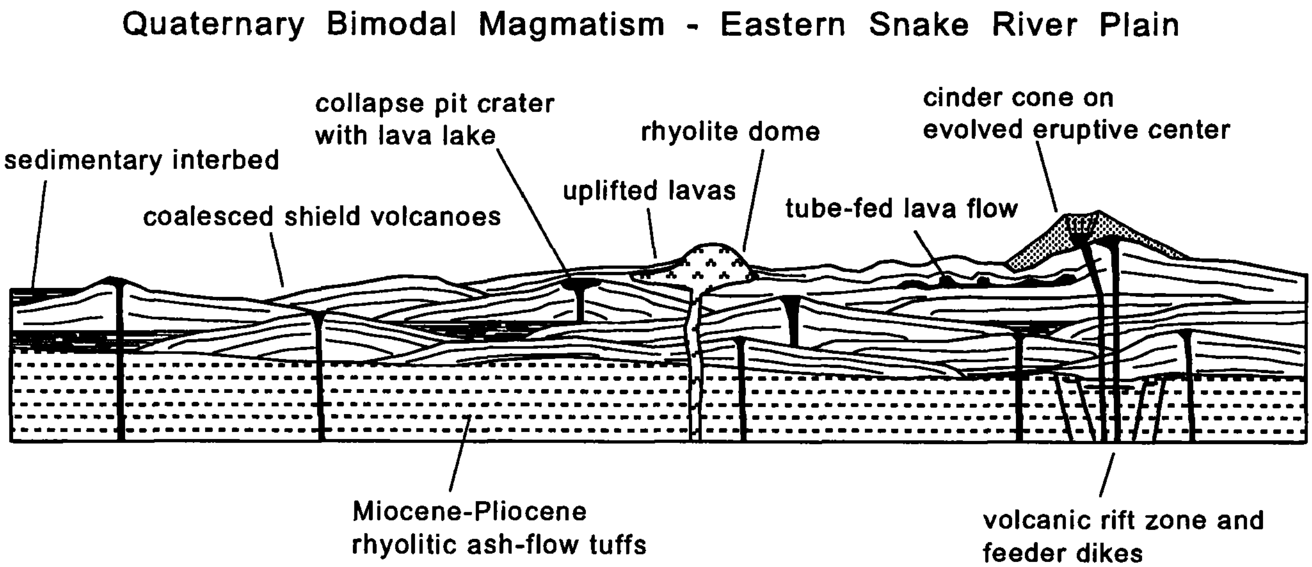

Figure 4. Schematic diagram of plains volcanism as developed on the eastern Snake River Plain. Modified from Greeley (1977), the diagram illustrates myriad magmatic and surficial processes that contribute to the evolution of the province.

magma is stored beneath ESRP eruptive centers in narrow elongate sill and dike networks perpendicular to the direction of least compressive stress. Fracture systems related to regional horizontal extension allow magmas to locally penetrate all levels of the lower and middle crust along a vertically-oriented dike system.

This scenario implies that ESRP extension-related magmatism is comparable to that measured or inferred at active basalt rift systems although the mechanisms of extension may differ somewhat. Dikes in Hawaii and Iceland are emplaced as blade-like structures propagating laterally from a magma reservoir (Rubin and Pollard, 1987) as the crust is inflated and extended around the chamber. Whether or not an eruption ensues, fissures may form on the surface if dikes are sufficiently shallow. A horizontal component of magma injection, whereby magma migrates along the length of a fissure during or prior to vertical ascent, may occur in some dikes associated with rift zones on the ESRP. Non-eruptive fissures and grabens (Kuntz et al., 1988, 1994) that extend beyond the edges of Holocene volcanic fields and away from their eruptive centers may be related to lateral dike propagation away from the eruptive part of the fissure as well as vertical dike propagation above the reservoir. The combined vertical and lateral propagation results in surface deformation shown in Fig. 6 as a general scenario of ESRP dike and reservoir geometry based on the perspectives of Rubin and Pollard, Kuntz (1992), and Hackett and Smith (1992). It should be noted that lateral magma migration is highly speculative and that surface features observed on the ESRP could result from variable amounts of magma ascent from an tabular reservoir. As a dike ascends into overlying basaltic layers, the extension above the advancing dike produces nested grabens providing low topographic areas for lava accumulation as magma erupts on the surface. Lava partially or wholly covers the depressed region as it flows over non-eruptive segments of the fissure system.

Perhaps the most important factor in the style of ESRP magmatism, and its dependency on crustal extension, is a relatively low magma supply rate which is manifested in numerous small monogenetic eruptive centers rather than large complex shields. Compared to regions of high eruption rates, such as Hawaii or Iceland where shield tumescence due to magma injection is followed by deflation during an eruption, ESRP subsurface reservoirs do not have significant readjustment during an eruption. This results in short-lived low-volume eruptions because a progressive pressure drop occurs as the reservoir is depleted (Kuntz, 1992). ESRP eruptions terminate at a critical pressure level a relatively short time after the eruption begins.

Tectonic influences are also reflected in chemical compositional variations in ESRP volcanic rocks. Although the system has been described as being "bimodal" (rhyolite and basalt), there are clearly intermediate compositions. Major element chemical trends (Fig. 7) demonstrate that the evolved eruptive centers produce a wide range in compositions without significant break between end-members. Detailed discussions of ESRP petrology (e.g. Leeman, 1982b; Leeman et al., 1976, 1985; Kuntz et al., 1985; 1992) indicate complex processes related to source heterogeneity, fractionation of primary magmas, and crustal assimilation that are responsible for the diversity among ESRP

Figure 5. East flank of Pillar Butte, the eruptive spatter and block vent for the Holocene Wapi lava field, surrounded by a lava lake that was produced during collapse and infilling of the vent area.

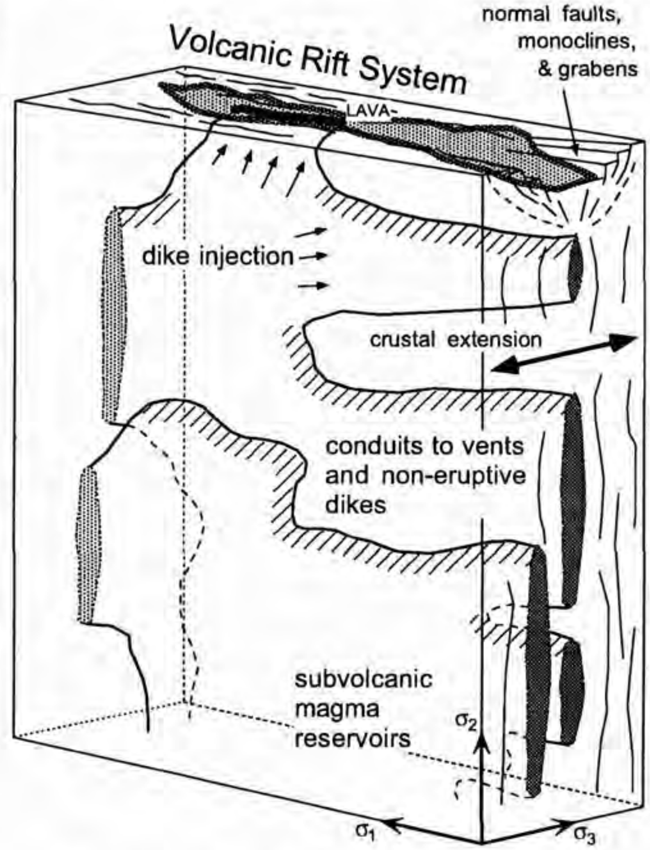

Figure 6. Schematic model of blade-like dike emplacement on the eastern Snake River Plain. Lateral propagation is possible when the fracture toughness of the country rock is exceeded by magma pressure. Orientation of dikes and vertical reservoirs are controlled by the regional stress field. Adapted from Rubin and Pollard, 1987; Kuntz, 1992; and Hackett and Smith, 1992.

volcanic rocks. Intermediate chemical and lithologic compositions are typically found in evolved eruptive centers such as Cedar Butte volcano (Stop 8) and Craters of the Moon lava field (Stop 10).

PETROLOGY OF CEDAR BUTTE VOLCANO: IMPLICATIONS FOR QUATERNARY HIGH-SILICA RHYOLITE MAGMATISM ON THE EASTERN SNAKE RIVER PLAIN

Michael McCurry,
Idaho State University, Pocatello, ID
Karl Hayden,
11917 East Archer Pl., Aurora, CO
William R. Hackett,
WRH Associates, Salt Lake City, UT
S. Mertzman,
Franklin & Marshall College, Lancaster, PA

Cedar Butte is a unique, geochemically "evolved" volcanic center located in the axial volcanic zone of the eastern Snake River Plain (abbreviated ESRP, Fig. 1). Lavas and pyroclastic rocks at this center span an essentially continuous compositional spectrum from ~54 to 75% SiO_2 (Hayden et al., 1992; Hayden, 1992). Although geochemically and petrologically similar to other evolved volcanic centers on the Snake River Plain (abbreviated SRP; Leeman, 1982b; Kuntz et al., 1986; Stout et al., 1994), none of those has produced such highly siliceous magmas. Cedar Butte therefore provides a critical link between the evolved mafic to intermediate volcanic centers which occur on many parts of the SRP (e.g., Craters of the Moon), and the young (< 2 Ma) high-silica rhyolite domes, sills and flows of the ESRP (Spear, 1979; Spear and King, 1982; Kuntz and Dalrymple 1979, Kuntz et al., 1992a; Hackett and Smith, 1992).

Here we summarize major geological and geochemical features of the center, and describe some implications of these data for evolution of late-stage (Leeman, 1982a; Hildreth et al., 1991) high-silica rhyolites of the ESRP. Classification of our lithologic units follows the recommendations of the IUGS Subcommission of Systematics of Igneous Rocks (Le Bas et al., 1986).

Geology

Some aspects of the following discussion follow from reconnaissance-scale work by Spear (1979), and Kuntz and Kork (1978) and the detailed work (1:12,000) of Hayden (1992). Cedar Butte volcano is a ~400 ka (Kuntz et al., 1994) polygenetic volcanic center located near the intersection of two major structural lineaments, the Arco Rift Zone and ESRP axial volcanic zone (Fig. 1). The volcano (Stop 8) consists of a broad shield, ~4 by 9 km across and

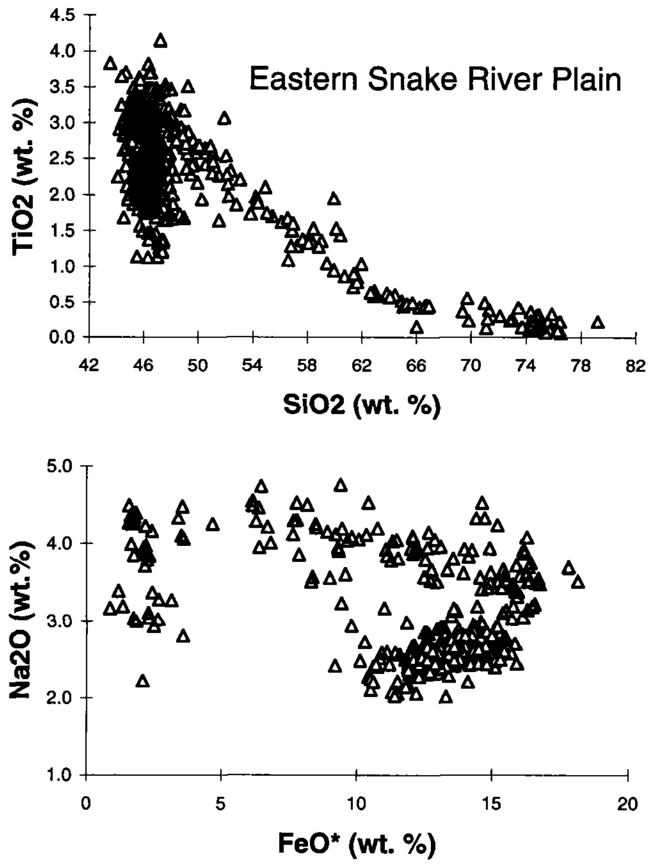

Figure 7. Covariations in Na_2O vs. FeO and TiO_2 vs. SiO_2 for ESRP compositions ranging from basalt to rhyolite. Data are from numerous sources including Leeman, 1982b,c, Kuntz et al., 1992, Hayden, 1992; Fishel, 1993, Spear, 1979; Spear and King, 1982; Leeman et al., 1985, Hildreth, et al., 1991, Stout and Nicholls, 1977; Knobel et al., 1995, Reed et al.,1997; and Hughes, unpublished data.

120 meters high, a prominent ~1-km-long curvilinear spatter rampart, and a large, 100-meter-high compound tephra cone (Fig. 8). Vents and dikes are north-northeast to northwest trending and are concentrated near the center of the shield.

This seemingly modest-sized shield is slightly elongate to the northwest, covering an area of ~31 km^2, with a minimum volume of erupted material of 9.2 km^3 (Hayden, 1992). Much of the volcano is probably buried by later Pleistocene to Holocene lavas, however. Lava flows which appear to have been derived from Cedar Butte have been identified in the subsurface from cores and borehole logs (Hayden, 1992; Spear, 1979; Steve Anderson, U.S. Geological Survey, personal communication, 1994). Similar lavas also are present in an uplifted block of basalt on the east side of Big Southern Butte (Fishel, 1993). These observations suggest the volcano had a roughly equant distribution, radiating ~20 km from the central part of Cedar Butte (Hayden, 1992). Cedar Butte volcano may therefore have had a total volume of exceeding 10 km^3—comparable to that of the largest "evolved" center on the Snake River Plain, Craters of the Moon volcanic center (Kuntz, et al., 1986).

Cedar Butte evolved through five major stages of activity (Fig. 8).

Stage 1: Effusion of a roughly north-trending high-silica rhyolite lava flow ~3 km long, 1 km wide and at least 70 meters thick (volume ~0.2 km^3). The flow is mantled by blocky and pumiceous breccia. Phenocrysts are sparse (<1% total volume) and consist of sanidine > fayalite > quartz > Fe-Ti oxides and accessory zircon and apatite.

The southern toe and eastern margin of the flow are relatively steep, giving Cedar Butte an unusual step-like morphology on those sides (outlined as a scarp on Fig. 8). In previous mapping of the region (Kuntz and Kork, 1978; Kuntz et al., 1992a, 1994; Spear, 1979) the east side of the butte was mapped as a north-trending fault scarp; one of very few faults on the ESRP. However, we reinterpret this scarp as a steep flow lobe margin of the underlying rhyolite. Although the rhyolite is mostly covered by a thin veneer of younger basaltic trachyandesite flows, it is exposed through nearby "windows" not covered by subsequent lava flows (Hayden, 1992). Some of the younger flows erupted from vents on top of the rhyolite; in these areas the later lavas are contaminated with xenoliths and xenocrysts of the rhyolite (near "fissure vent" on Fig. 8). Excellent exposures of these flows along the scarp demonstrate that they flowed over the scarp, rather than being cut by it. Therefore faulting either predates the younger flow, or, we believe more likely, the scarp was produced by edge of the underlying rhyolite flow.

Stage 2: The apparent passive effusion of the stage 1 rhyolite flow was followed by more explosive eruption of trachydacite lava. Explosive fountaining is suggested by the flows' generally distinctive clastogenetic textures. Orientations of stretched vesicles, glass ribbon bomb orientations, and rheomorphic fold axes indicate the lava erupted from a vent that is now buried under the stage-3 tephra cone. The lava is sparsely porphyritic; phenocryst abundances and assemblage resemble those of the preceding rhyolite.

Stage 3 is distinguished by the construction of a large tephra cone. The cone is one of the largest Quaternary tephra cones on the ESRP. It has a relief of ~100 meters, is 1.2 km across, and is deeply eroded, suggesting it was originally even larger. A large breach on the north side of the cone appears to be erosional rather than volcanic in origin.

In contrast to other large tephra cones on the SRP (Womer, et al., 1982; McCurry et al., this volume), Cedar Butte is distinguished by an absence of evidence for meteoric water involvement. Eruptions appear to have been

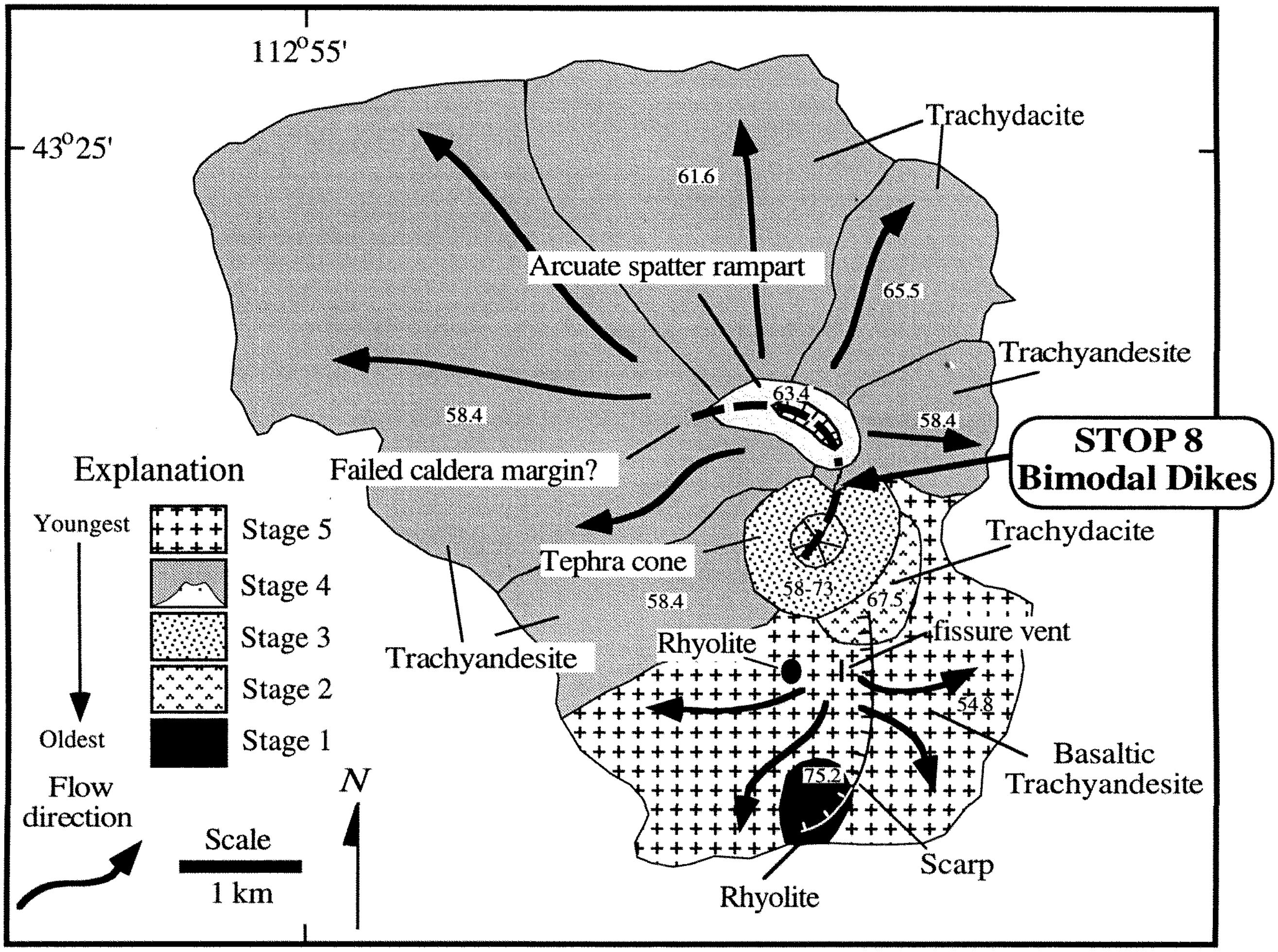

Figure 8. Diagrammatic illustration of the major geologic units of Cedar Butte volcano. Stages are discussed in the text. Flow directions are inferred from stretched vesicle lineations and flow fold orientations (modified from Hayden, 1992 and Hackett and Smith, 1992).

dominantly strombolian in nature, having produced thick layers of moderately to poorly bedded and moderately to poorly sorted scoria bombs, pumice, and spatter. Most exposures are of moderately welded agglutinate. Small lava flows also issued from the sides of the cone.

The cone-forming eruptions produced a spectrum of magma types (trachyandesite–trachydacite–rhyolite), as well as pyroclasts containing intermingled glasses of contrasting compositions. In our preliminary work we did not observe a correlation between stratigraphy and composition, at least on the scale of 5–10 meters of stratigraphic section. However exposures are very limited, so we can not rule out larger scale patterns which would indicate a correlation between time and chemical composition of the erupted materials.

Spear (1979) suggests that the large tephra cone was the last phase in formation of Cedar Butte. However, good exposures on the north flank of the cone indicate that flows to the north pinch out rapidly south against the cone, rather than project beneath the cone.

A spectacular en-echelon system of north-northeast-trending compositionally-bimodal dikes cuts through the extreme northern flank of the tephra cone (Fig. 8). These are described in the discussion for Stop 8.

Stage 4: After tephra cone formation ceased (stage 3), effusive activity shifted north. Subsequent eruptions were voluminous and took place from a north to northwest curvilinear fissure system at least several hundred meters to perhaps 1-km long, producing a prominent arcuate spatter rampart (Fig. 8). When combined, dikes, tephra cone, and arcuate vent zone define a near-circular 150° arc with a radius of curvature of ~0.8 km (bold dashed line on Fig. 8).

Geometry of the curvilinear dike/fissure system resembles vent/dike systems which are influenced by interactions between local (i.e. volcano-related) and regional stress fields (e.g., Mueller and Pollard, 1977). However, at Cedar Butte, this would imply a regional extension directed perpendicular to the plain, an idea which is inconsistent with the orientations of northwest-trending normal faults marginal to the plain. We speculate that the distinctive geometry of this system of vents resulted from incipient caldera formation above a shallow magma chamber (e.g., see discussions in Suppe, 1985, p. 223–228).

At least five distinct eruptions from the arcuate vent zone produced lavas ranging from trachyandesite to trachydacite in composition (Fig. 8). Although individual lava flows appear to be relatively homogeneous, some exhibit varying scales of magma mixing and hybridization (Fishel, 1992).

The lavas are typically sparsely porphyritic. Intermediate flows contain phenocrysts of plagioclase, olivine, ferroaugite, Fe-Ti oxides and accessory apatite. More felsic flows contain phenocrysts of plagioclase + anorthoclase + olivine + Fe-Ti oxides and accessory zircon and apatite. Accessory xenocrysts and wispy blebs of contrasting magma types (i.e. small-scale magma mixing) are fairly common but not abundant. In contrast to highly evolved lavas at Craters of the Moon (abbreviated COM; e.g. Stout et al., 1994) we found no accidental lithic fragments which might have been derived from dissaggregated Precambrian basement.

Stage 5: The final eruption at Cedar Butte produced the least siliceous lava (54.8% SiO_2). The vent is a north-trending fissure just south of the tephra cone (Fig. 8). The eruption produced a relatively thin flow which mantles much of the southern third of Cedar Butte. Although similar in most respects to older trachyandesites at Cedar Butte, this flow contains scattered xenoliths and xenocrysts of "stage-1-type" rhyolite, consistent with our interpretation of a large subsurface extent for the rhyolite flow.

No significant erosion occurs between lava flows or pyroclastic units suggesting there was no major hiatus during formation of the volcanic center. Unfortunately, exposures are very limited due to weak erosional incision of the young rocks, and we have no basis for quantifying the time of evolution.

The five stages of Cedar Butte evolution record a systematic change over time from more siliceous to less siliceous eruptive products. This relationship between composition and time, combined with abundant evidence for magma mixing and partial hybridization at Cedar Butte, suggest that the lavas were erupted from a shallow, compositionally zoned magma chamber.

Geochemistry

Major element chemistry: Cedar Butte is a moderately alkaline intermediate to silicic volcanic center (Hayden, 1992 and Spear, 1979). Major geochemical features are illustrated in several Harker diagrams (Fig. 9). In these figures SRP olivine tholeiite basalts and COM lavas are shown for reference.

Lavas and pyroclastic rocks span a nearly continuous spectrum of major-element composition from 55 to 75% silica. Major- and trace-element covariation plots (Fig. 9) exhibit smooth variations in chemistry which are most often linear (e.g., Ca and FeO*), but also include some moderate (e.g., K_2O, Rb) and pronounced changes in slope (Ba, Zr).

Salient aspects of Cedar Butte rock chemistries are as follows (also refer to Fig. 9):

1. There is a pronounced compositional discordance between the most mafic Cedar Butte rocks and SRP olivine tholeiite basalts. This discordance is characteristic of other mafic to intermediate volcanic centers on the SRP, such as Craters of the Moon (e.g., Leeman, 1982b; Stout et al., 1994). Cedar Butte is missing the most mafic compositions observed at COM.
2. Cedar Butte rocks overlap in composition with other evolved volcanic systems on the ESRP (represented in Fig. 9 by COM). It seems remarkable that essentially all major chemical, petrologic and mineralogical features of Cedar Butte rocks overlap with COM rocks between 54 and 66% SiO_2, despite the difference in ages and locations of the two centers (e.g., Stout et al., 1994; Hayden, 1992). Clearly, the evolution of the two suites must be due to the same processes. There are some differences, perhaps best demonstrated in Fig. 9 by an apparent discordance in Zr-contents of Cedar Butte and COM. Trends of Zr-contents of both volcanic systems seems to define straight lines; respective trends appear offset and of opposite slopes between ~57 and 65% silica. Over this range Zr-concentration increases from ~1,300 to 1,900 ppm in COM rocks, while declining from ~3200 to 1,900 ppm in Cedar Butte rocks.
3. Some changes in slopes defined by chemical variation trends correlate systematically with changes in phenocryst assemblage and abundance (as previously demonstrated for COM rocks). Most prominent among these are changes in trends of Rb, Ba, and K_2O. At a bulk silica content of ~60%, the Rb-trend increases in slope, whereas Ba changes from positive to negative slope with increasing silica. The changes correlate with the appearance of intratelluric alkali-feldspar (Fig. 10). Barium strongly partitions into alkali-feldspar, whereas Rb is mildly incompatible. Therefore it seems likely that fractionation of this phase produced the observed opposite behaviors of the two elements.

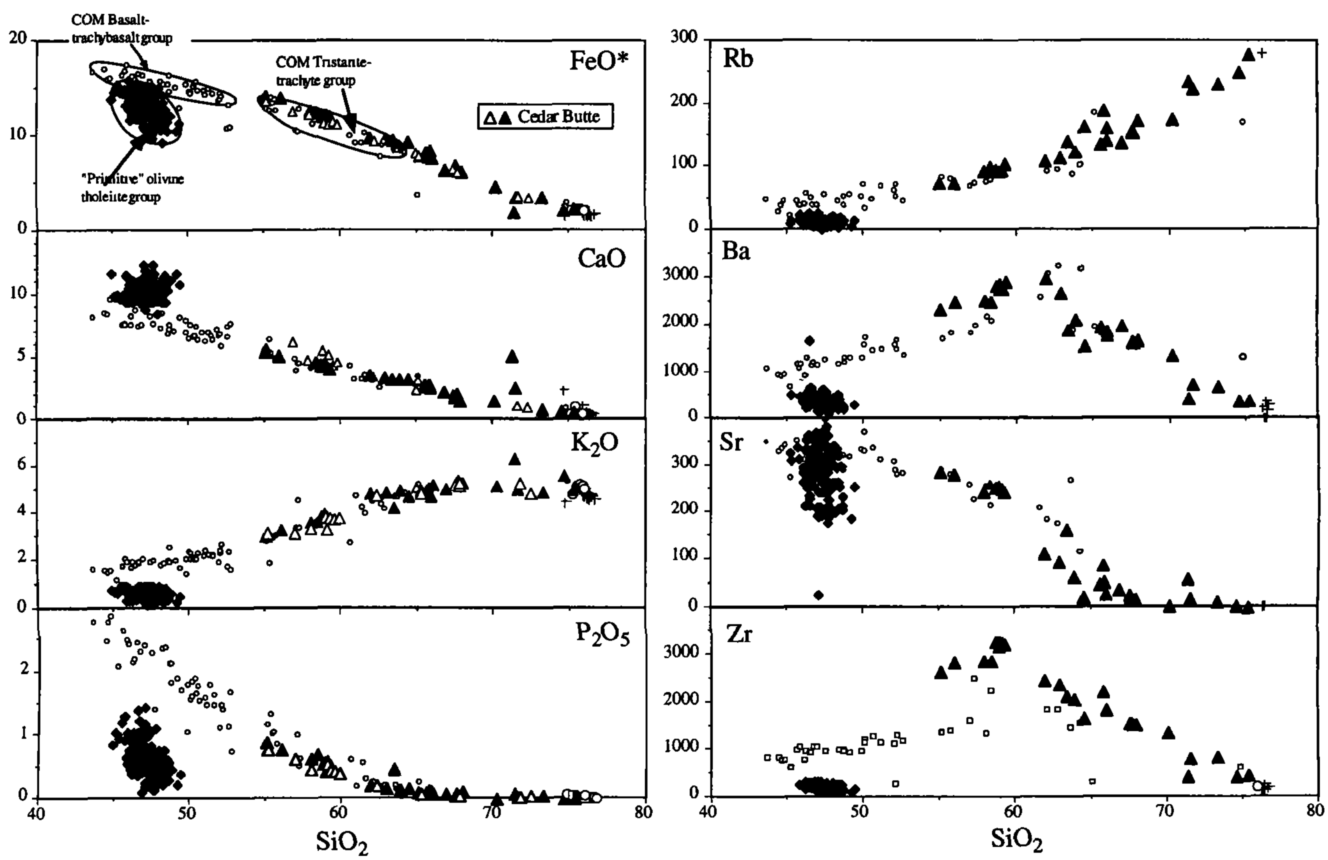

Figure 9. Representative whole-rock major and trace element analyses of Cedar Butte and related volcanic rocks; oxides normalized to 100% on an anhydrous basis (Hayden, 1992; McCurry, unpublished data). Symbology and sources of the data are as follows: large filled triangles = Cedar Butte; small open triangles = Cedar Butte (Spear, 1979); small diamonds—Snake River plain olivine tholeiite basalts (Kuntz et al., 1992a; Spear, 1979, Fishel, 1993); small open circles—"evolved" volcanics of Craters of the Moon volcanic center (Kuntz et al., 1992a; Leeman et al., 1976); plus symbol—Big Southern Butte rhyolite (Spear, 1979; unpublished data by McCurry and Mertzman); large open circle—East Butte rhyolite (Spear, 1979).

A second significant change in trend is demonstrated by a flattening of K_2O-silica slope at ~67% SiO_2 on the Harker diagrams. This roughly coincides with an increase in the abundance of alkali feldspar and decline, and eventual absence, with increasing silica, of plagioclase as an intratelluric phase.

The curved nature of some Cedar Butte covariation trends precludes simple two-component mixing as a major petrogenetic mechanism, although as previously stated, petrographic and field evidence for at least some magma mixing is strong. Stout et al., (1994), Reid (1995), Leeman et al., (1976) and Leeman (1982b) convincingly demonstrated that similar lavas at COM were largely the products of fractional crystallization. The basis of arguments they brought to bear at COM is essentially the same at Cedar Butte.

4. Perhaps the most significant feature of chemical data from Cedar Butte is that they appear to close a "compositional gap" (between ~66 and 74% SiO_2) between trachyandesite-dacite lava sequences and high-silica rhyolites of the ESRP. Rocks spanning this compositional range erupted during at least two stages of volcanic center evolution (stages 2 and 3). Samples which were analyzed are only sparsely porphyritic, and olivine and alkali-feldspar phenocryst compositions are intermediate between mafic and silicic extremes. Therefore it seems unlikely that the bulk rock chemistry is an artifact of crystal accumulation or magma mixing, and opens up the possibility that the most siliceous rocks are genetically related to the intermediate rocks (cf. Spear, 1979).

Hayden (1992) performed incremental mass balance calculations of fractional crystallization using observed compositions of phenocrysts, and produced a close match to the observed trends in bulk major element rock chemistry ($\Sigma r^2 < 0.5$; Bryan et al., 1968). Spear (1979) performed

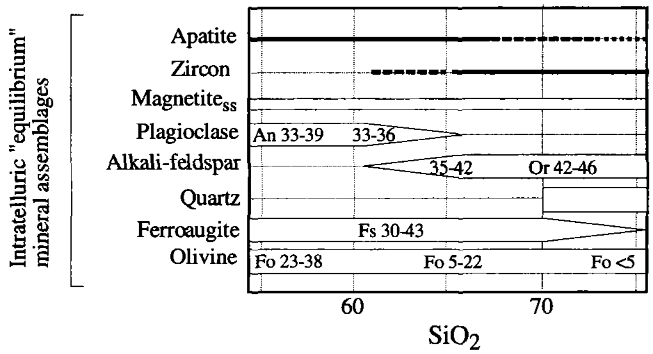

Figure 10. An interpretation of assemblages of minerals which, based upon their petrographic features, are believed to be intratelluric phases which were in equilibrium with the host magmas. Widths of bars indicates relative abundance. Numbers on bars indicates compositions of respective phases based upon electron microprobe analyses (Hayden, 1992).

similar calculations over a smaller silica range. He also presents chondrite-normalized REE data which support a fractional crystallization model. However he specifically excluded rhyolites from this model because: 1. the most silicic rocks have lower LREE concentrations than some intermediate rocks; 2. absence of a fractionating phase which could have produced the lower LREE ratios.

Our preliminary REE analytical work, illustrated in Fig. 11, confirms the patterns of LREE and HREE shown by Spear. Note that Big Southern Butte (BSB), made of rhyolite even more evolved than the most silicic rhyolite at Cedar Butte, has even lower LREE/HREE ratios than rhyolites at Cedar Butte. Fractionation of small amounts of allanite or monazite may have produced the observed REE behavior (McCurry, unpublished data). We have observed rare small phenocrysts in thin section which could be allanite and are in the process of obtaining heavy mineral separates from Cedar Butte rhyolites to confirm or rule-out presence of the phase.

Isotope chemistry: Sr- and Nd-isotopes of four Cedar Butte samples are illustrated in Fig. 12. Analyses are also shown of samples of high-silica rhyolites from East Butte and Big Southern Butte.

Samples from Cedar Butte range from 0.70684 to 0.70967 in initial $^{87}Sr/^{86}Sr$ ratio; ε_{Nd} varies from –4.14 to –4.70. Sr- and to a lesser extent, Nd-isotopes correlate systematically with silica content. Simple two-component mixing has already been excluded on the basis of bulk major element chemistry and patterns of phenocryst assemblages and composition. A coupled assimilation and fractional crystallization (AFC) model illustrates one possible relationship (Fig. 12). The most mafic trachyandesite is assumed to represent the parent magma. Plagioclase+alkali feldspar, olivine, ferroaugite, Fe-Ti oxides and allanite are assumed to fractionate in weight proportions of 0.6, 0.15, 0.15, 0.10, and $3x10^{-5}$, respectively, yielding estimated bulk distribution coefficients of D_{Sr} = 4 and D_{Nd} = 1.1 (McCurry, unpublished data). Assimilant chemical composition is from lower and upper crustal xenoliths in SRP lavas (Leeman et al., 1985). The long curved line represents the AFC model fractionation path. Small numbers indicate percentage crystallization of the parent magma.

The AFC model yields a successful match for observed Sr- and Nd-isotopes as well as Sr- and Nd-concentrations. It is highly sensitive to r (ratio of assimilation to crystallization). No successful models were produced using r's of more than a few percent, primarily because of the extremely low Sr-concentration of the most evolved sample (2.6 ppm). This apparently rules out more than a few percent contribution from any reasonable crustal rock.

Sr-isotope, compositional and textural features of COM rocks suggest greater involvement of crustal material (e.g., Leeman et al., 1976; Stout et al., 1994). For example, whereas accidental crustal xenoliths are common in COM lavas, they are absent at Cedar Butte. In addition, COM Sr-isotopes increase from 0.7079 to 0.7117 between 45 and 63.5% silica, Cedar Butte Sr-isotope ratios increase from 0.7068 to 0.7097 between 55 to 75% silica. Differences in silica and Sr-isotope patterns of the two systems are illustrated in the inset to Fig. 12.

One of the intriguing features of the isotopic data for high-silica rhyolites of the ESRP is that, with the exception of one sample from Cedar Butte, all overlap in Nd- and Sr-isotopes with SRP olivine tholeiite basalts and overlap with each other in major- and trace-element chemistry (Figs. 9, 12). This suggests that a repeating mechanism of formation is involved for the rhyolites, different than that which produced earlier Tertiary rhyolites in the same area (e.g. Leeman, 1982a,c). The isotopic data appear to preclude any mechanism involving major contribution to the rhyolites from lower or upper crustal geochemical reservoirs (Fig. 12), and provides strong evidence of a liquid-line-of-descent, by fractional crystallization, between olivine tholeiites—intermediate magma suites—and high silica rhyolites.

Discussion

Intensive work on evolved volcanic centers of the eastern Snake River Plain has resulted in development of a strong argument for the origin of mafic-intermediate composition evolved volcanic rocks involving extreme fractional crystallization of and minor assimilation by a primitive olivine tholeiite parent (e.g., Thompson, 1972a,b, 1975; Leeman et al., 1976, 1982b; Stout et al., 1994; Kuntz et al., 1986; Reid, 1995). However high-silica rhyolite flows and hypabyssal intrusions, which overlap with the intermediate centers in

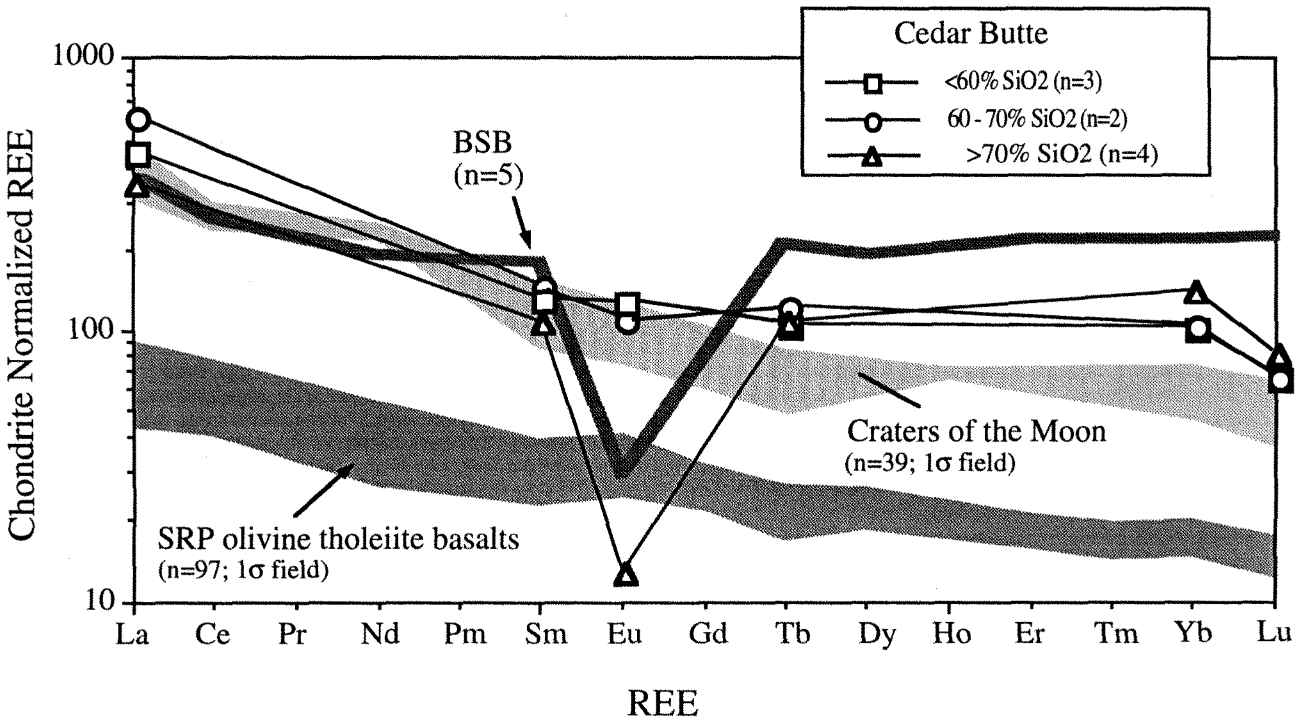

Figure 11. Chondrite-normalized REE plots of rocks from Cedar Butte (McCurry, unpublished data), SRP olivine tholeiites (medium shade pattern), COM lavas (light shade) and Big Southern Butte rhyolite (dark shaded line). Data for COM lavas and olivine tholeiites are from Kuntz et al., (1992a), Knobel et al., (1995), Fishel (1993) and Hughes (unpublished data). Data for Big Southern Butte are from Spear (1979) and Noble et al., (1979). Chondritic values from Anders and Ebihara (1982).

space and time, have been placed into separate, and somewhat poorly defined categories (e.g., "residual melt," Spear, 1979; crustal melt, Leeman, 1982c, Kuntz, 1992b).

We suggest that the rhyolites were produced by an extension of the same basic mechanism responsible for the other "evolved" magmas on the plain, i.e. extreme polybaric fractional crystallization of SRP basalt. This idea has previously been ruled out on the grounds of paucity of intermediate composition rocks, discordances in isotopic compositions (Leeman, 1982c), and trace element patterns (Spear, 1979). Although these arguments clearly apply to older Tertiary rhyolites of the ESRP (Leeman, 1982c), they do not apply as well to the younger rhyolites (i.e. Cedar Butte, Big Southern Butte, East Butte, etc.). Cedar Butte appears to be one place where the entire range (above 54% silica) of evolved magma compositions happened to be erupted. Most of the rhyolites overlap in Sr- and Nd-isotopes with SRP olivine tholeiites, and, finally, discrepancies in LREE data may be accounted for by fractionation of trace amounts of a mineral such as allanite or monazite.

Until we have documented an appropriate LREE-bearing mineral phase, the fractionation model is considered only a working hypothesis. However, if true this process has significant implications for late Quaternary magmatic evolution of the ESRP, because the volumes of high-silica rhyolite are significant. Big Southern Butte alone has an exposed volume of 8 km^3 (Kuntz et al., 1992a) and may have a total volume of 10–20 km^3 when subsurface volume is taken into account. This would imply existence of a large crustal parental basaltic magma reservoir perhaps ten to a hundred times that size. If located in the mid- to lower crust a chamber of that size might conceivably be still partially molten.

THE MENAN VOLCANIC COMPLEX

Gregory C. Ferdock,
Mackay School of Mines,
University of Nevada, Reno, Nevada
William R. Hackett,
WRH Associates, Salt Lake City, Utah

The twin cones of the Menan Buttes (Fig. 13) are part of a six-vent, late-Pleistocene complex of basaltic tuff cones and smaller tuff rings, aligned along a 5-kilometer, northwest-trending eruptive fissure west of Rexburg, Idaho. Recent work on the Menan volcanic complex includes Creighton (1982, 1987), Ferdock (1987), Hackett and Morgan (1988), and Kuntz et al., (1992).

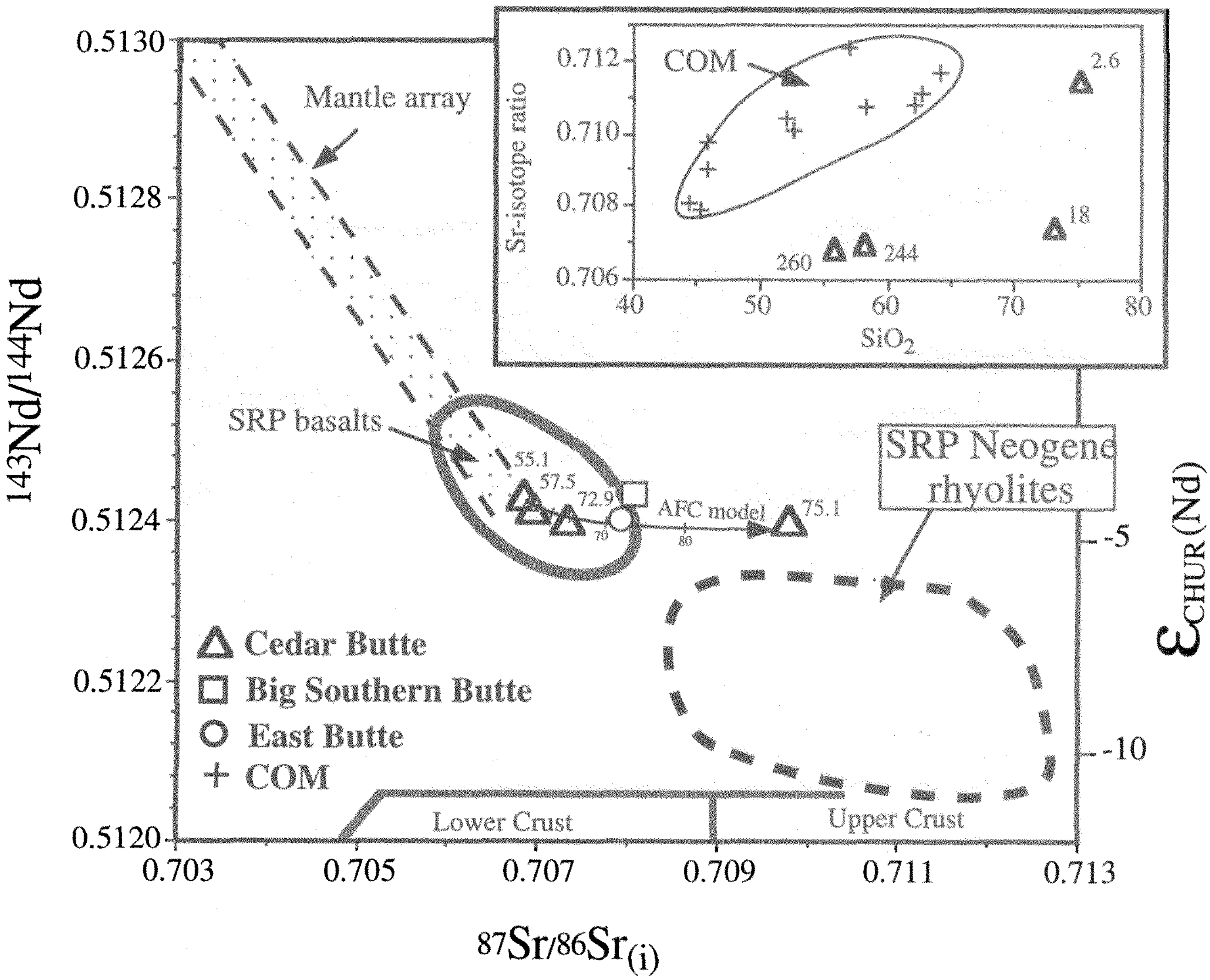

Figure 12. A plot of Nd- and Sr-isotope ratios for samples from Cedar Butte (McCurry, unpublished data); Cedar Butte (triangles), Big Southern Butte (open square) and East Butte (open circle). Numbers next to Cedar Butte samples are silica contents of the respective samples. Curved line represents an AFC model; numbers next to tick marks on the curve indicate percent fractionation of the trachyandesite parent magma (discussed in the text). Inset diagram illustrates relationships between Sr-isotopes and silica for COM (after Leeman et al., 1976) and samples from Cedar Butte. Numbers next to Cedar Butte samples are whole-rock Sr-concentrations. Fields for Neogene rhyolites and SRP basalts are based upon data from Menzies et al., (1983), Lum et al., (1989), and Hildreth et al., (1991).

The hydrovolcanoes of the Menan volcanic complex (Stop 3) were formed during the ascent of a basaltic dike into near-surface, water-saturated alluvial sediment and basaltic lava flows of the Snake River Plain aquifer, producing large volumes of palagonite tuff. The north and south Menan Buttes tuff cones are the largest features of the volcanic complex, composed of massive to thin-bedded, tan, lithified palagonite lapilli tuffs containing minor accidental clasts of dense basalt and rounded quartzite pebbles. The monotonous palagonite tuffs of the Menan Buttes tuff cones are the products of steady-state hydrovolcanic eruptions of wet basaltic tephra, generated during dike emplacement into the shallow aquifer. In the later stages of cone construction, steam explosions were situated above the aquifer and within the recycled tephra-slurry of the central craters, as shown by the paucity of accidental-lithic clasts derived from the underlying alluvial sediment.

Near-vent deposits of the Menan Buttes tuff cones are massive and poorly sorted, suggesting mass emplacement as slurry flows of wet, cohesive tuff. Along the rims of the craters, original bed forms are obscured by dense palagonitization of the tephra. Cone-flank deposits are planar-

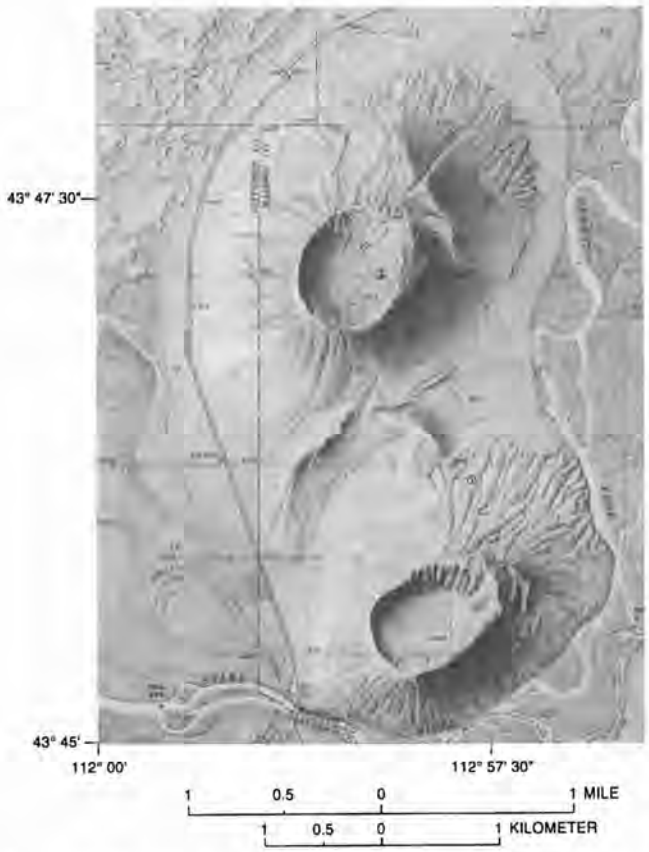

Figure 13. Portion of the shaded relief map (Menan Buttes, Idaho, U.S. Geological Survey, 1951, 1:24,000 scale shaded topographic map) of the Menan Buttes tuff cones on the Eastern Snake River Plain. Phreatomagmatic eruptions occurred near the confluence of the Henrys Fork and the South Fork of the Snake River.

and cross-stratified, moderately sorted palagonite tuffs with local armored-lapilli beds, suggesting deposition as fall, surge and sheet wash. Deformation of the wet, cohesive tuffs occurred during or soon after deposition, as shown by monoclines, complex folds and possible detached slide blocks on the lower flanks of the tuff cones. Distal deposits beyond the cone flanks are fine, planar-laminated, palagonitic fall-out tuffs that were dispersed mainly to the northeast.

The North and South Little Buttes are eroded tuff rings situated along the eruptive fissure about 5 km south of the Menan Buttes. In contrast to the Menan Buttes tuff cones, the tuff rings are smaller, have lower slope angles, and the deposits are strongly cyclic with abundant quartzite pebbles derived from the underlying permeable alluvium. The cyclical nature of the eruptions is indicated by two distinctive classes of bed sets. Scoriaceous lapilli tuffs occur in coarse, planar bed sets, and were emplaced mainly as fall and minor surge deposits, during relatively "dry vent," violent strombolian eruptions. Intercalated with the scoriaceous deposits are bed sets of tan, cross-stratified, fine palagonite tuffs, emplaced as fall and surge deposits during relatively "wet vent" surtseyan eruptions, and driven largely by the flashing of external water to steam. Groundwater was probably always available during feeder-dike intrusion, and the alternating strombolian and surtseyan bed sets therefore suggest a fluctuating elevation of the magma column; such variation in magma pressure is commonly observed during historical basaltic eruptions. At the Little Buttes, vesiculating basaltic magma episodically reached the land surface, sealed itself from the incursion of external water, and erupted mainly coarse, scoriaceous ejecta. During periods of magma withdrawal, steam explosions occurred within saturated alluvium above the shallow dikes, producing fine palagonitic tuffs containing up to 50 percent quartzite clasts.

GEOLOGICAL HAZARDS AND SURFICIAL PROCESSES

Richard P. Smith,
Idaho National Engineering and Environmental Laboratory, Idaho Falls, ID
William R. Hackett,
WRH Associates, Salt Lake City, UT

Geologic investigations of seismic and volcanic hazards at the Idaho National Engineering and Environmental Laboratory (INEEL) have been underway for several decades. Much of the recent work has been concentrated on recent displacement on Basin and Range faults north of the INEEL, processes operating in volcanic rift zones within and near the INEEL, and stratigraphy and structure beneath the surface of the ESRP near INEEL. Specific investigations include paleoseismology of faults, structural geologic mapping of faults, detailed mapping of volcanic rift zones, regional geophysical surveys, high-precision geodetic surveys to measure crustal deformation, deep drilling, and heat flow analysis.

For most INEEL facilities, the seismic hazard is dominated by the Basin and Range normal faults north of the ESRP. These faults are capable of magnitude 7 or greater earthquakes and have recurrence intervals of thousands to tens of thousands of years. Facilities at INEEL have been designed and constructed to withstand the effects of ground motions associated with potential earthquakes on the southern ends of these faults.

The most significant volcanic hazard for INEEL facilities is inundation by lava flows, but the hazard from ground deformation (fissuring and tilting) due to shallow dike intrusion and from volcanic gases has also been evaluated (Hackett and Smith, 1994). The probability of inundation by lava flows increases towards volcanic rift zones and the axial volcanic zone. For any particular facility the probability is less than 10^{-5} per year, most likely in the range of

10^{-6} to 10^{-7} per year. Impacts from ground deformation and volcanic gases are even lower. The hazard due to seismicity associated with dike intrusion and volcanism is less than the hazard due to seismicity due to tectonic processes (Smith et al., 1996). The INEEL seismic network, with stations deployed in volcanic rift zones on the ESRP and along major faults in the Basin and Range province, is operated to monitor tectonic seismicity and to warn of impending volcanic or intrusive activity.

Surficial Processes

Although tectonic and volcanic processes produce the gross geomorphic characteristics of the ESRP, late Pleistocene to late Holocene surficial processes, including glacial outburst flooding (Stop 11), range fires, and eolian erosion and deposition (overview at Stop 5) contribute significantly to the geomorphic appearance of the ESRP. The effects of glacial outburst flooding along the Big Lost River include scouring of loess cover from basalt lava flows, formation of large gravel bars and boulder trains, deposition of exotic gneissic and granitic boulders on basaltic terrain, excavation of cascades in basalts, and possible modifications to canyons in basalt bedrock (Rathburn, 1991, 1993). Some of these features will be seen at field trip Stop 11 (on Day 3).

During the Pleistocene, extensive eolian deposition produced thick loess blankets on the ESRP and in adjacent areas of southeastern Idaho (Pierce et al., 1982). Eolian processes, aided by range fire denudation of large tracts of the ESRP, have continued to modify the landscape up to the present time. Prominent lineaments on the ESRP, observed in landsat imagery and aerial photography, are the result of eolian redistribution of surficial materials following range fires (Morin-Jansen, 1987). That process has been observed in action during the last few years, and will be discussed in detail at field trip Stop 5 (on Day 2).

HYDROGEOLOGY OF THE IDAHO NATIONAL ENGINEERING AND ENVIRONMENTAL LABORATORY

Steven R. Anderson,
U.S. Geological Survey, Idaho Falls, ID
Scott S. Hughes,
Department of Geology, Idaho State University,
Pocatello, ID

Facilities at the INEEL are used in the development of peacetime atomic-energy applications, nuclear safety research, defense programs, and advanced energy concepts. Liquid radionuclide and chemical wastes generated at these facilities have been discharged to onsite infiltration ponds and disposal wells since 1952; use of disposal wells was discontinued in 1984. Liquid-waste disposal has resulted in detectable concentrations of several waste constituents in water in the Snake River Plain aquifer underlying the INEEL (Barraclough et al., 1976; Bartholomay et al., 1995). Detailed stratigraphic studies using outcrops, cores, and geophysical logs are being conducted to evaluate the relations between the geologic framework and the movement of water and waste in the unsaturated zone and aquifer.

Water runoff from valleys north of the ESRP follows drainages such as the Big Lost River, Little Lost River and Birch Creek to enter an extensive groundwater system beneath the INEEL (Fig. 14). The unsaturated zone and aquifer are composed of a 500-m thick sequence of discontinuous volcanic and sedimentary deposits of Pleistocene age. Individual basalt lava flows are characterized by large zones of irregular fractures and voids (Barraclough and others, 1976) creating high hydraulic conductivities. Groundwater travels southwest through the volcanic sequence and discharges mainly through highly conductive zones of basalt along the Snake River at Thousand Springs (approximately 35 km northwest of Twin Falls) which is over 200 km southwest of the recharge zone.

Stratigraphic units underlying the INEEL include mainly basalt and sediment. Basalt units, which make up about 85 percent of the volume of deposits in most areas, include individual flows, flow groups, and supergroups (Lanphere et al., 1994; Anderson et al., 1996; Welhan et al., 1997; Wetmore et al., 1997). A basalt flow group is a sequence of basalt flows such as the Hells Half Acre and Wapi lava fields that erupted within a relatively short period of time from a single fissure or series of vents related to a common magmatic system (Kuntz et al., 1980, 1994). These units represent eruption episodes that lasted from days to years. A basalt supergroup is a group of flows that cannot be separated into individual flow groups on the basis of available well data, usually because most wells involved were not cored for paleomagnetic, petrographic and geochemical studies. These units represent multiple eruptive events over thousands of years. Different amounts of intercalated lacustrine, playa, and fluvial sediment lenses and eolian soil blankets occur between flow groups and supergroups; the amount of sediments depends on both the sedimentation rate and the repose interval between eruptions at any given site.

Although many flow groups are locally separated by lenses of fine sediment ranging from a few centimeters to tens of meters in thickness, contacts between some groups apparently have little or no sediment or soil development. The overall profile of ESRP shields and the locations of vents (Figs. 4,14) indicate control by shield construction on direction of streams and location of sedimentation (Hughes et al., 1997). This is evident in the position of Big Lost River and Birch Creek playas in a sediment trough near TAN

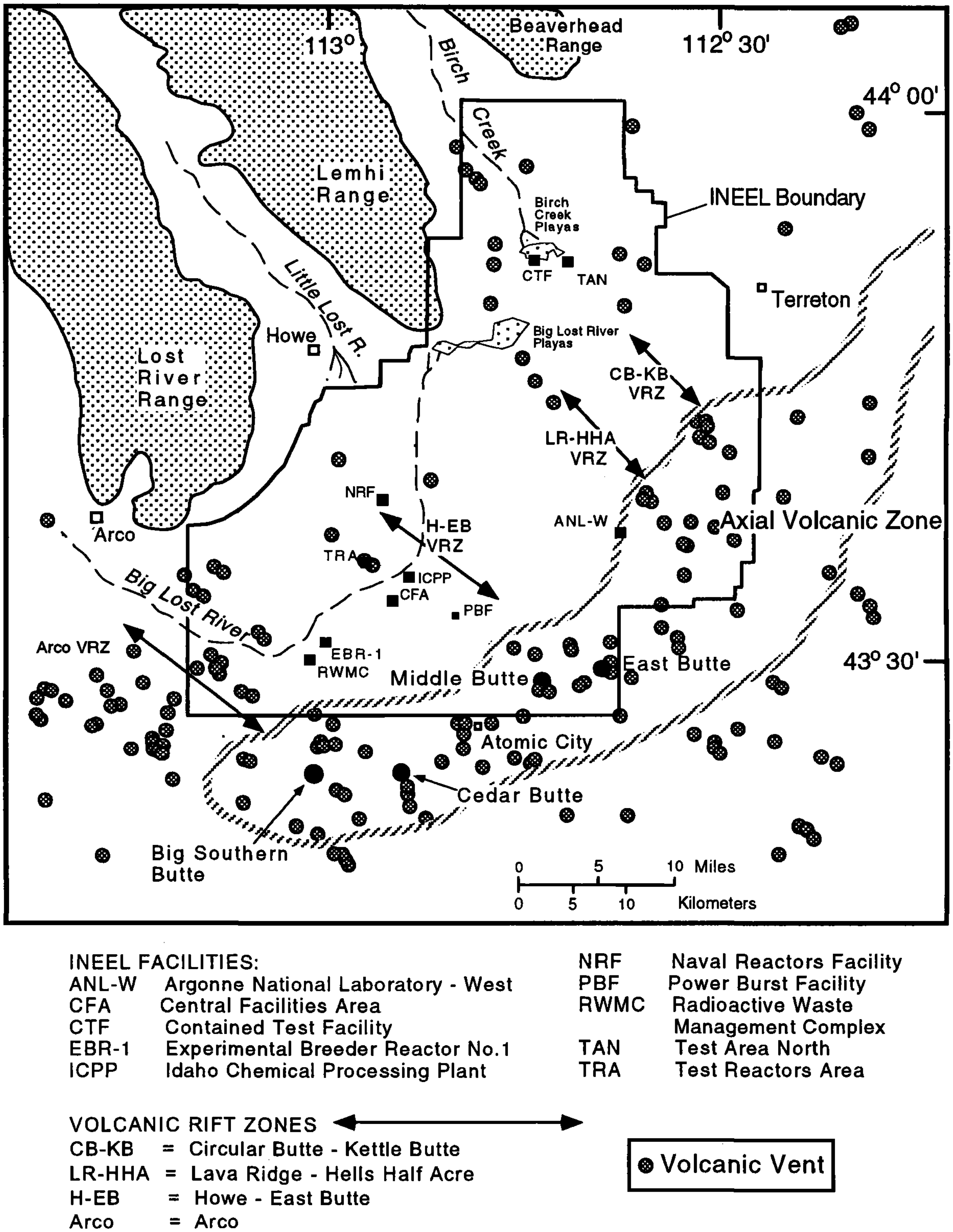

Figure 14. Map of the Idaho National Engineering and Environmental Laboratory (INEEL) on the eastern Snake River Plain, illustrating locations of volcanic vents related to the axial volcanic zone and Quaternary basaltic vents. Double arrows depict volcanic rift zones (see text for explanation).

(Gianniny et al., 1997). The trough corresponds to an apparent paucity of eruptive shields along a NE-SW corridor through the INEEL (Kuntz et al., 1994). Volcanic vents apparently are restricted to the axial volcanic zone southeast of this corridor and along the northwest margin of the ESRP in the INEEL vicinity. Stratigraphic and lithologic studies of surface and subsurface sediments in the northern INEEL (Geslin et al.; 1997) suggest that buried Pleistocene depositional environments were similar to present day playa and fluvial systems, and were controlled by volcanic topographic highs. Many of these relations will be observed and discussed at Stop 5 on the field trip.

Basaltic lava flows, as major components of the ESRP aquifer system, have internal variations in hydraulic conductivity related to their thickness and to the dimensions and orientations of scoriaceous vesiculated zones, tension fractures, brecciated rubble zones, and flow surfaces. These factors control conductivity on scales ranging from a few cm to several m, and the directional variances caused by them are probably random throughout a lava flow. Hydraulic conductivity varies locally over one-million fold, with highest- and lowest-conductivity zones in basaltic breccia and sedimentary interbeds, respectively. Once a shield volcano is buried by younger lavas and sediments, the orientation of the conductive brecciated zones within lavas is controlled largely by the original depositional slopes. Groundwater flow is enhanced further in randomly oriented and irregular void spaces within the flow units. For example, Holocene shields, such as the Wapi and Hells Half Acre lava fields, contain a highly irregular plexus of flow channels, tubes, tumuli, collapse depressions and other surface irregularities, all of which could serve as aquifers once those shields are buried beneath the water table.

Identification and correlation of subsurface stratigraphic units rely mainly on direct and indirect measurements of basalt properties, including paleomagnetic polarity and inclination, radiometric age, petrographic characteristics, chemical compositions, and natural-gamma emissions of naturally-occurring K, U, and Th determined from borehole logging tools (Lanphere et al., 1994; Anderson and Bartholomay, 1995; Reed et al., 1997). At least 121 basalt-flow groups and 102 sedimentary interbeds have been identified at and near the INEEL (Anderson et al., 1996); however, many flow groups beyond the main facilities, where most cores and two-thirds of the wells are located, have been subsequently reassigned to supergroups on the basis of thickness distributions (Wetmore et al., 1997).

Complex controls by the basalt/sediment stratigraphy on the distribution of waste plumes have been identified near injection wells and waste ponds at the INEEL. Packer tests indicate stratigraphic control of an injected tritium plume in basalt flows of contrasting thickness at the Idaho Chemical Processing Plant (Morin et al., 1993; Federick and Johnson, 1996). The formation of perched groundwater zones at the Test Reactor Area is controlled by the distribution of basalt and thick sediment layers beneath waste ponds (Cecil et al., 1991). The distribution of basalt shields and inferred dikes associated with a volcanic rift zone may control an injected plume of trichloroethylene that is perpendicular to regional groundwater flow directions at Test Area North (Hughes et al., 1997).

FIELD TRIP GUIDE

Many of the stops in this field trip guide can be enhanced by extended visits and side trips. The roads are generally adequate throughout the early summer to late fall, but often impossible to travel during the winter and early spring. The first day of the field trip includes phreatomagmatic volcanism (Massacre Volcanic Complex, Menan Volcanic Complex) along the Snake River (Stops 1 and 3), Hells Half Acre lava field (Stop 2), and the relation of the ESRP to the Basin and Range province. Stops 4–9 on the second day will concentrate on the Axial Volcanic Zone of the ESRP and the geology of the INEEL. Topics will include silicic domes and INEEL geology (Middle and East Buttes, with discussions on surficial processes and hydrology), lava flow emplacement and basaltic shield growth (Table Legs Butte, Cerro Grande lava), compositionally evolved eruptive centers (Cedar Butte Volcano), and rift systems (North Robbers spatter vent). Stop 10 on the second day will be at Craters of the Moon lava field. The third day will allow observation of structural manifestations of basaltic magmatism and glacial cataclysmic flooding at Box Canyon (Stop 11), eruptive and non-eruptive fissure systems and lava lake formation at Kings Bowl (Stop 12), and Split Butte, a phreatomagmatic tuff ring formation (Stop 13).

Day One

1. Massacre Volcanic Complex (Bill Hackett and Scott Hughes)

West of Pocatello, the I-86 freeway roughly parallels the Snake River along the southern physiographic boundary between Basin and Range and Snake River Plain geologic provinces. Late Tertiary and early Quaternary volcanic rocks partly fill the intermontane valleys of the Basin and Range and lap onto their adjacent mountain flanks (Trimble and Carr, 1976). Downstream from American Falls, the Snake River cuts through late Miocene and early Pliocene rhyolite deposits that are overlain by a complex assemblage of Neogene basaltic tuffs and lava flows. The Neogene units were redefined by Luessen (1987) as the Massacre Volcanic Complex composed of the Eagle Rock, Indian Springs and Massacre Rocks basaltic pyroclastic subcomplexes, and the basalt of Rockland Valley (Fig. 15). The pyroclastic com-

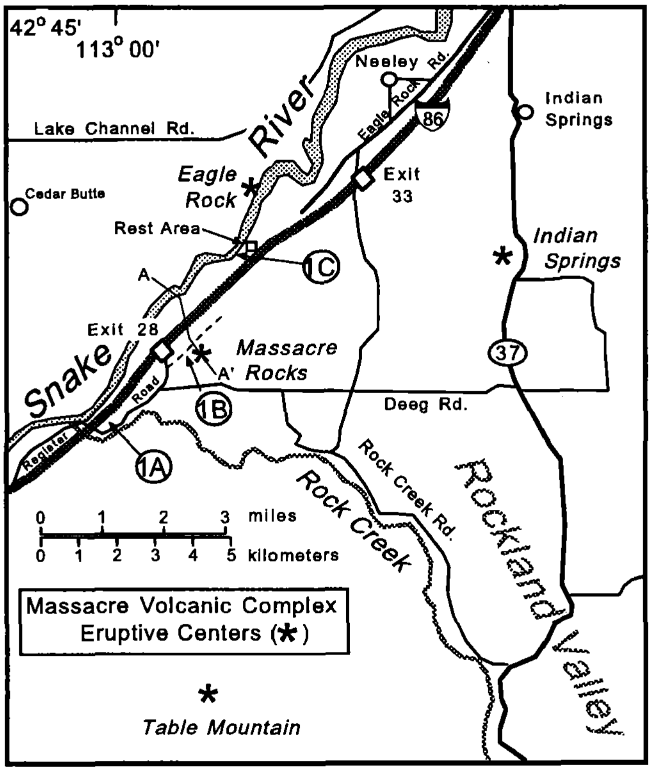

Figure 15. Map of the Massacre Rocks area with eruptive centers of the Massacre Volcanic Complex. Phreatomagmatic units of the Massacre Complex were overlain by Quaternary basalts that flowed north from eruptive centers in Rockland Valley. Field trip stops (1A–1C) are circled.

plex, which crops out over a 128 km^2 area about 15 km southwest of American Falls, was deposited during explosive phreatomagmatic eruptions along the Snake River. The Massacre Volcanic Complex overlies a sequence of unconformable volcanic and volcaniclastic deposits including (youngest to oldest) the Little Creek Formation, the Walcott Tuff, and the Neeley Formation (Fig. 16).

Drive east on I-86 freeway from Exit 21, which is east of the intersection of I-84 and I-86 (Fig. 1), to milepost 26 and proceed northeast to the Register Road overpass that is approximately 2 miles from Exit 28, the entrance to Massacre Rocks State Park. Stop 1A is in the roadcut on the southeast side of the highway immediately past the overpass (Fig. 15). At least two subhorizontal Quaternary basalt lava flows, which flowed northward down Rockland Valley from Table Mountain shield volcano, lap onto basaltic tuffs of the Massacre Rocks subcomplex that have a slight westward dip. Autoclastic basal breccia and baked paleosol occur between the two lava flows. The underlying unit is a stratified lithic tuff with subtle gas escape features that are perpendicular to the dip. These elutriation pipes, assuming they were originally vertical, possibly indicate post-eruptive tectonic tilting or local downwarping along the southern margin of the ESRP.

Continue on the freeway and take Exit 28; turn south and then immediately northeast on the frontage road for about one-quarter mile to Stop 1B (Fig. 15) which is on juniper-covered slopes about 0.5 km south of Massacre Rocks State Park. Hike up to one of the prominences about 100 m off the road to observe bedded tuff deposits and ballistic ejecta. The deposit is on the flank of the Massacre Rocks unwelded tuff cone (Fig. 17); block sags are common and reflect close proximity (less than 1 km) to the vent. Scour surfaces, well-stratified planar bedding and dunes indicate high flow velocities during volcanic surges which are fairly common in ESRP phreatomagmatic deposits.

Return to the freeway continuing northeast, take Exit 33 and re-enter the freeway headed southwest to the rest area near Massacre Rocks State Park. Walk southwest from the rest area parking lot along the paved path leading to the old Oregon Trail wagon ruts. The path forks and the paved part passes under the freeway to the Oregon Trail exhibit. Continue southwest on the unpaved path for about 100 m, leave the path and climb down the ridge toward the river to observe the stratigraphic section (Stop 1C). Table 3 illustrates the sequence that can be observed at this location. On the opposite side of the river can be observed Cedar Butte basalt, a Quaternary ESRP lava flow, and ignimbrite of the Massacre Volcanic Complex.

Return to the freeway, drive southwest and take Exit 28, re-enter the freeway and continue northeast toward Pocatello. Pillar Butte, the primary vent area for the Holocene Wapi lava field, and the shield profile can be observed to the northwest while driving on I-86 in this region. While driving northeast through the Neeley area about 2 miles upstream from the interstate rest area, a small shield volcano and several spatter cones can be observed on the north side of the river. This is a small vent area for Cedar Butte basalt (*not* the same petrologically evolved Cedar Butte eruptive center described in a previous section), a lobe of which impounded the river and formed American Falls Lake (Carr and Trimble, 1963). The basalt lobe, ~75,000 years old, is typical ESRP lava. The lake beds are very thick near here and the lava flows have been eroded by the Bonneville Flood. Rapids in the river are caused by a fault with small displacement, possibly related to dike intrusion associated with the Cedar Butte flows.

2. Hells Half Acre part 1 (Dick Smith and Scott Hughes)

Drive northeast on I-86 past Pocatello, and take I-15 toward Idaho Falls (Fig. 1). Drive past the town of Blackfoot, cross the Snake River, and continue for approximately 8 miles past milepost 101 to Stop 2 which is at the rest area constructed on the Hells Half Acre lava field. Several trails

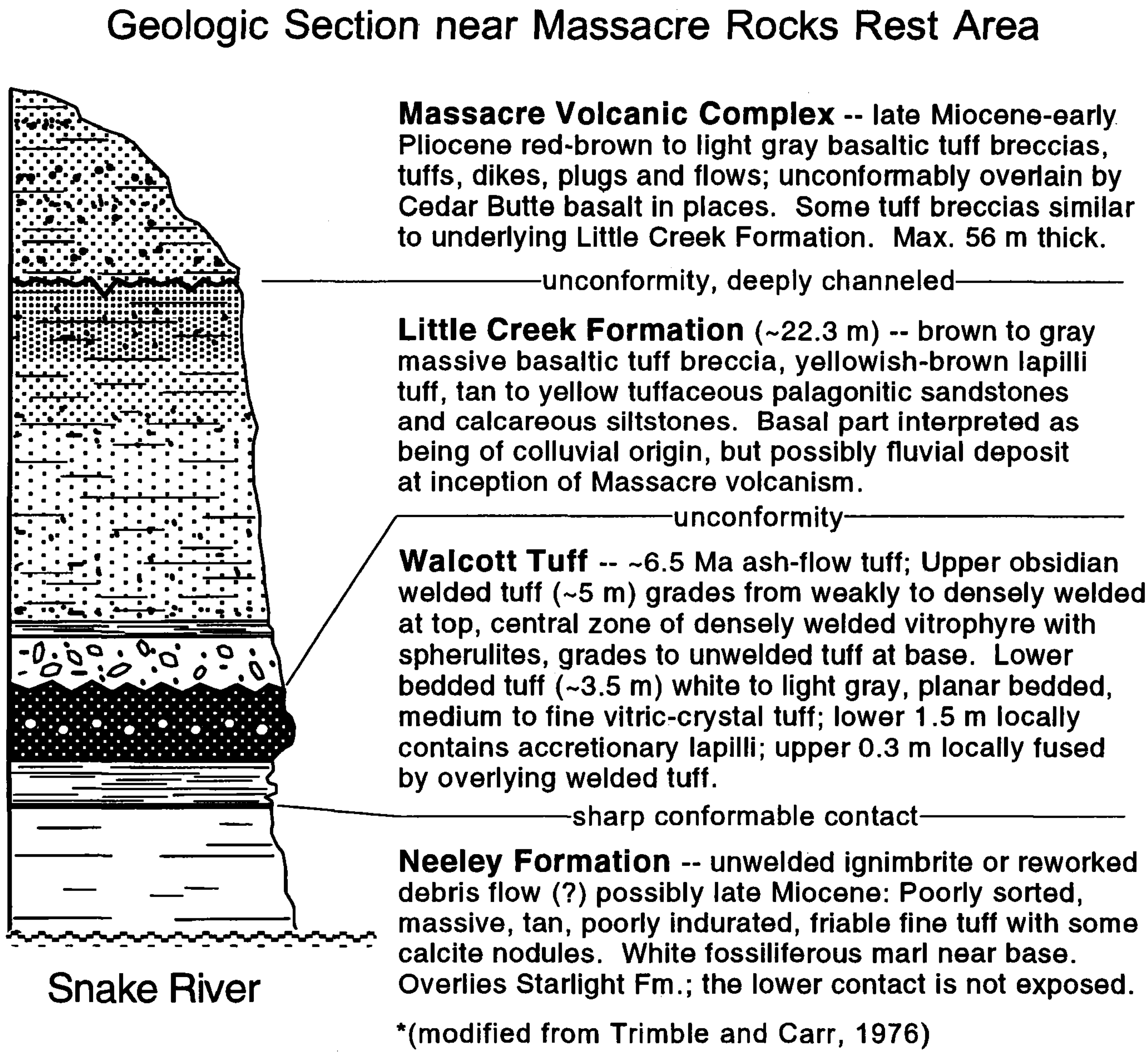

Figure 16. Geologic section at Stop 1C (access from interstate highway rest area near Massacre Rocks) illustrating sequence observed along the Snake River. Refer to Fig. 15 for location of this and other stops in the Massacre Volcanic Complex. Adapted from Trimble and Carr (1976).

are available to allow easy access to the highly irregular (several meters of relief) surface of this Holocene lava field. Most of the ESRP basalt flows were emplaced as tube-fed pahoehoe lavas characterized by numerous collapse depressions (Greeley, 1982). These flows had relatively low viscosity, low width-to-length and low thickness-to-width ratios, and were emplaced as coalescing lobes fed from a central molten interior. Flow lobes were relatively thin and volatile-rich as they emerged from the vent and became thicker and degassed with time and distance from the vent. ESRP flows developed small (<1m—several m scale) gas cavities immediately upon eruption in the form of shelly pahoehoe, and layers of solid basalt on the upper and lower surfaces which were subject to breakage, rafting and formation of brecciated zones. Many flows exhibit a stream-fed component within self-constructed levees of chilled basalt.

Pahoehoe lavas normally have numerous squeeze-out areas where molten lava extrudes through cracks in the surface, thus leading to an irregular surface with up to several meters of relief. At the flow front, pahoehoe lobes grow from

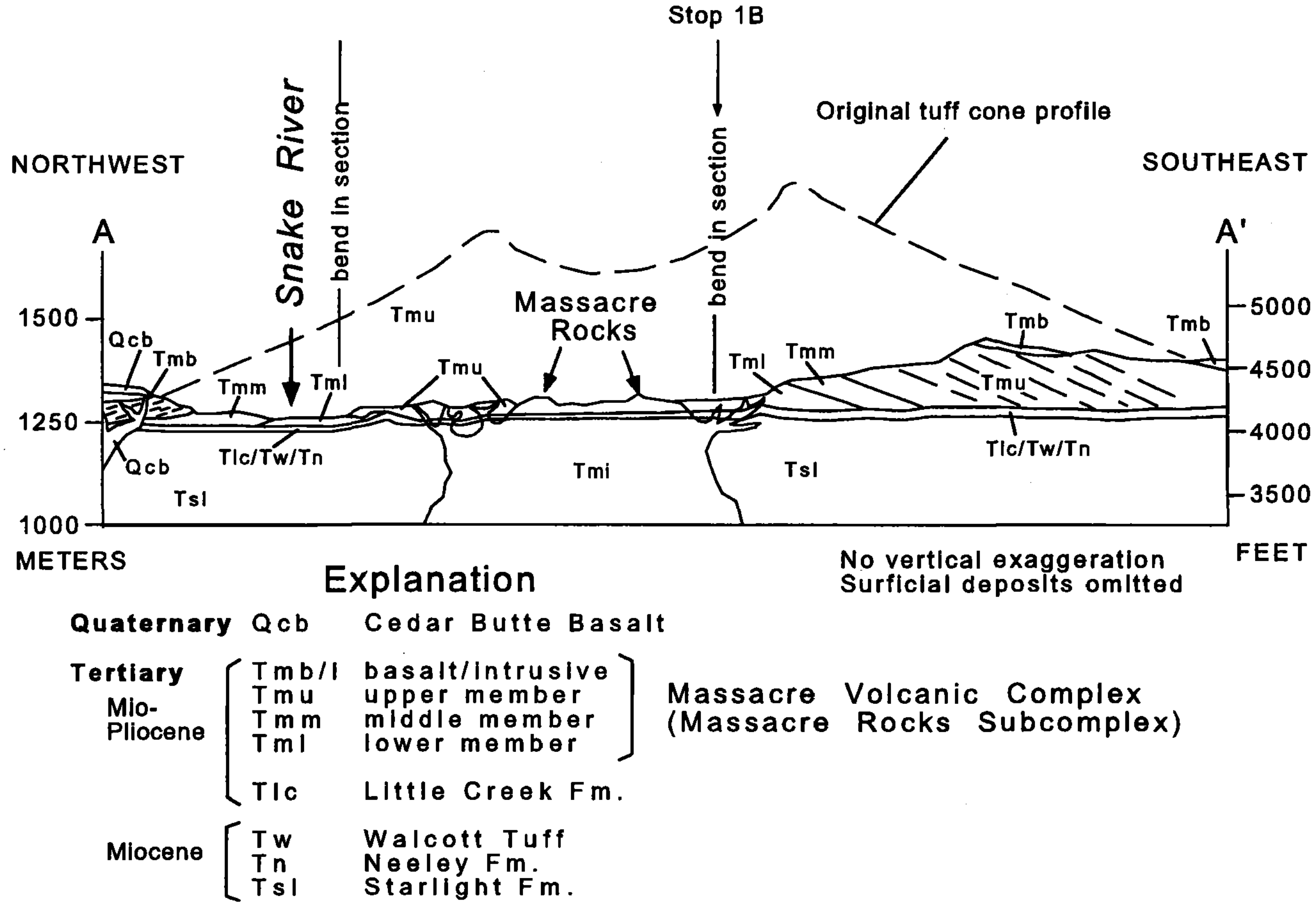

Figure 17. Geologic cross-section of the Massacre Volcanic Complex (after Luessen, 1987) through the Massacre Rocks eruptive center. Refer to Figure 15 for the location of the A-A' cross-section line.

initial breakouts by either (1) pushing the lobe upward and away from a slow-moving lobe front, or (2) forward expansion as the crust rolls under a fast-moving lobe front (Keszthelyi and Denlinger, 1996). Thin sheet pahoehoe flows, which are not well-represented on the ESRP, have individual lobes typically less than a meter to several meters across. Sheet flows such as those in Hawaii (Hon et al., 1994) have an initial thickness of a few tens of centimeters, but the thickness increases dramatically to several meters as magma pushes from within, inflating and lifting the surface.

The morphology of ESRP Holocene lava flows, such as those of Hells Half Acre, indicates that medial to distal parts of flows experienced inflationary emplacement styles, but at a much larger scale than that which is typical of Hawaiian pahoehoe lavas. Flow fronts can be as thick as several meters and pahoehoe "toes" several tens of meters across; flow lobes 5–8 m high and ~100 m wide are common. As magma breaks out from an expanding lobe, dramatic deflation results in a basin-like sag of the interior and deep tension fractures (3–5 meters deep) along the periphery of the lobe. The collapse increases the irregularity of the flow surface and the number of fractures. A typical ESRP lava flow facies cross-section (Fig. 18) indicates significant variation in thickness due to collapse.

3. Menan Volcanic Complex (Bill Hackett and Greg Ferdock)

Drive north on I-15 freeway and take Exit 119 at Idaho Falls, and continue northeast on Highway 20. Turn west on Highway 80 about 8 miles south of Rexburg—reset odometer to 0.0—and travel west towards Annis and Menan. Drive through the town of Annis and at mileage 3.6 bear right onto a narrow paved road along the northeast edge of Little Buttes (Fig. 19). At mileage 4.1, turn left into quarry for Stop 3A. The Menan Buttes are known to many geologists because they have been used in topographic map exercises of popular introductory laboratory manuals. They are outstanding morphological examples of tuff cones (see Hackett and Morgan, 1988 for detailed discussions).

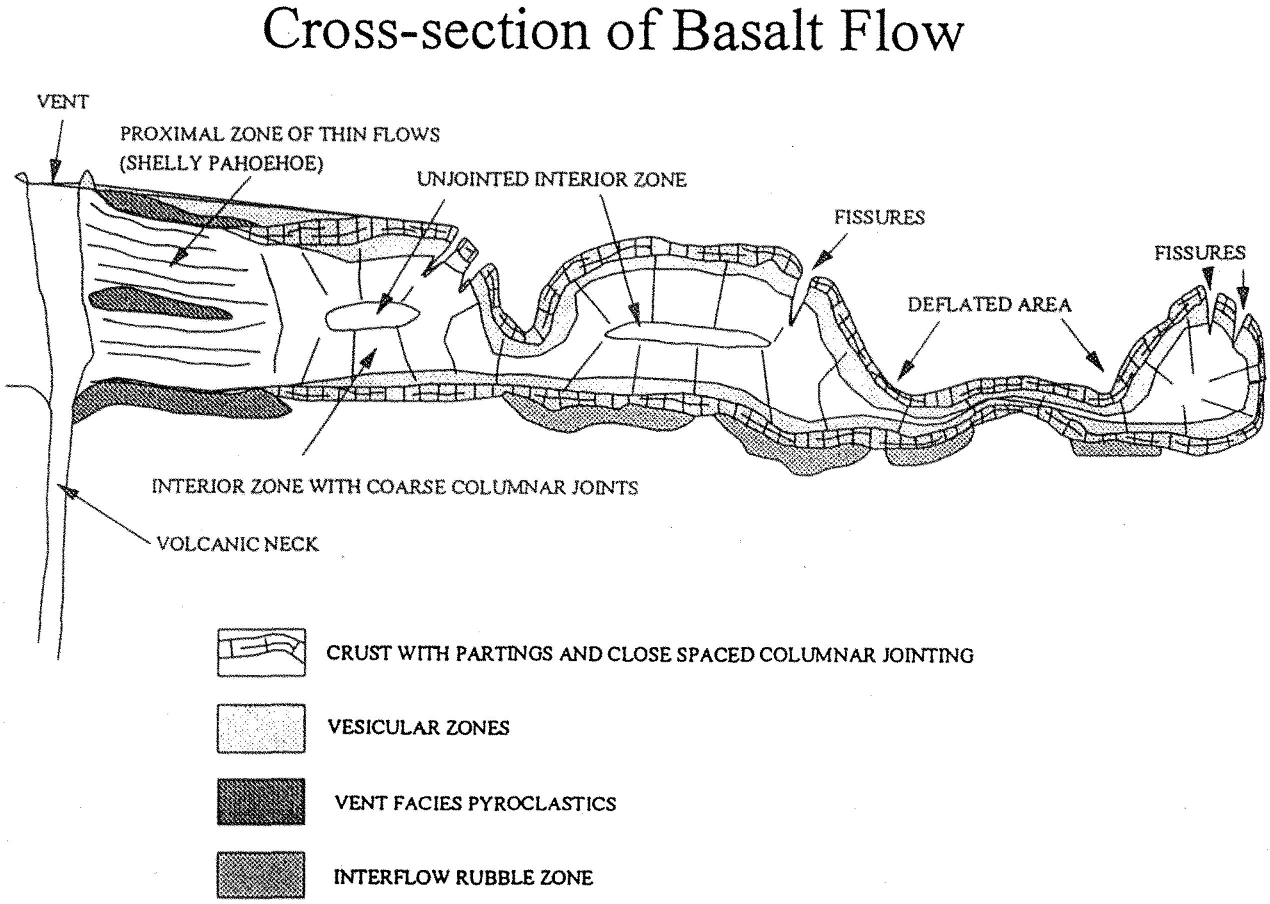

Figure 18. Schematic cross-section of an eastern Snake River Plain basalt flow. The diagram illustrates the inflation-deflation style of pahoehoe lava emplacement typical of ESRP flows, and the irregular surfaces developed during flow and cooling. Flow fronts are typically greater than 5 m thick and the inflated pods range from a few meters to over 100 m across. Adapted from an original unpublished drawing by Richard P. Smith; redrawn version provided by Allan H. Wylie, Lockheed-Martin Idaho Technologies, Inc.

A few miles south of the Menan Buttes are the remnants of two tuff rings, the North and South Little Buttes, which are much smaller and have lower slope angles than the two tuff rings. The deposits are strongly cyclic and contain abundant accidental quartzite pebbles derived from the underlying permeable alluvium. The tuff rings are dominated by two types of bed sets: black, planar-bedded, coarse scoriaceous lapilli tuff bed sets (mostly fall, with minor surge deposits) were formed during relatively "dry vent" violent strombolian eruptions driven by rapid vesiculation. Intercalated bed sets of tan, cross-stratified, fine palagonite tuffs (fall and surge deposits) were formed during relatively "wet vent" surtseyan eruptions driven by phreatomagmatic processes.

From Little North Butte quarry—reset odometer—head west on road 400N. Turn left (north) at mileage 1.9 on road 400W and drive toward the Snake River. Cross the bridge (mileage 3.7) and at mileage 5.1 turn right (east) onto the unmarked, improved gravel road that heads northeast, between North and South Menan Buttes. At mileage 6.0 turn left onto an unmarked road towards the south flank of North Menan Butte and park at mileage 6.2 for Stop 3B. Walk up the gully to observe excellent tuff exposures and, if time permits, reach the southern crater rim where densely palagonitized tuffs and large ballistic blocks are exposed.

The Menan Buttes tuff cones are the largest features of the Menan volcanic complex, with reconstructed volumes of 0.7 (North) and 0.3 (South) km^3. Dense basalt volume equivalents are 0.4 and 0.2 km^3, respectively. They are among the largest terrestrial tuff cones, with volumes comparable to those of Diamond Head, Oahu, and Surtsey, Iceland. Deposits of the North and South Menan Buttes tuff cones are monotonous, massive to thin-bedded, tan, lithified palagonite lapilli tuffs with minor xenoliths of dense basalt and rounded quartzite pebbles. At this stop observe

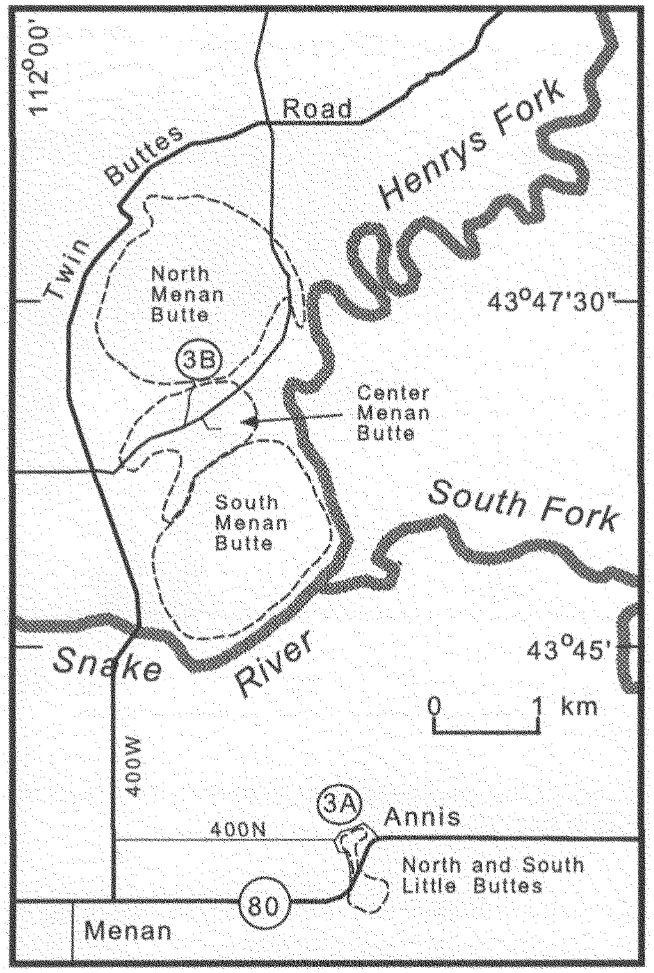

Figure 19. Index map of the Menan Buttes phreatomagmatic tuff cones with field trip stops (3A, 3B). The Menan Volcanic Complex includes North, Center and South Menan Buttes (3B), as well as North and South Little Buttes (3A). Compare to Fig. 13.

weakly convoluted, thin-bedded tuff, and bed forms that are nearly obliterated by palagonitization. This is the last stop of the first day.

Day Two

4. Hells Half Acre—part 2 (Dick Smith and Bill Hackett)

Drive west on Highway 20 from Idaho Falls, start mileage at I-15 overpass, and continue west-northwest for 20 miles to Twentymile Rock where the road curves broadly around the lava field toward the southwest. Noting mileage, turn left (southwest) on the first unpaved road after the curve, remain on the road closest to the lava field where it forks (about one mile), and continue for a total of 2.6 miles from the highway to Stop 4 (Fig. 20) along the margin of the lava field. The vent area of the Hells Half Acre lava field is located in the northwest part of the lava field, and lies only 3 miles southeast of this stop. It is a northwest-elongated crater containing several deep collapse pits. A northwest trending eruptive fissure, located just south of the crater (Kuntz et al., 1994) and short sections of eruptive fissures located between the crater and this field trip stop suggest that the feeder system for the lava field is a northwest-trending dike. This is consistent with the observation that ESRP volcanic rift zones trend northwestward, almost perpendicular to the trend of the plain itself (Kuntz et al., 1992), and to the interpretation that dike orientation in the ESRP is controlled by the same northeast-trending extension stress field that produces Basin and Range faulting adjacent to the ESRP (Hackett and Smith, 1992; Smith et al.,1996).

At this stop, two sets of non-eruptive fissures, flanking the eruptive fissure, extend northwestwardly from beneath the edge of the Hells Half Acre volcanic field (Kuntz et al., 1994). A several-meter-thick loess blanket that underlies the lava field obscures much of the fissuring, but in several places the loess has collapsed into the fissures and/or has been eroded into the fissures by percolating or flowing water. The fissure sets, separated by a distance of about 1 mile, were caused by a zone of extensional stress above the non-eruptive part of the dike and are typical of surface deformation associated with shallow dike intrusion in volcanic rift zones (Fig. 6), (Pollard et al., 1983; Rubin and Pollard, 1988; Rubin, 1992; Smith et al., 1996). Fissure widths are generally less than 1 meter, and the fissure walls are very irregular because pre-existing columnar jointing in the lava flows controlled the near-surface fissure shape. Parallel sets of non-eruptive fissures (well-known in Iceland, Hawaii and Galapagos) are also observed along the Great Rift between Kings Bowl lava field and the Craters of the Moon lava field (Kuntz et al., 1988) and in the Arco volcanic rift zone (Hackett and Smith, 1994). In addition, a small graben (~300 meters across, ~10 meters of vertical displacement, and several km long) occurs in the northern part of the Arco volcanic rift zone. We will visit this graben at field trip Stop 11 (day 3).

5. Idaho National Engineering and Environmental Laboratory—Middle and East Buttes (Dick Smith, Bill Hackett, Steve Anderson and Mike McCurry)

Return to Highway 20 and continue west past the radio tower on the south side of the road, and approximately 2 miles past the boundary of the INEEL turn left (south) onto an unpaved road to East Butte for Stop 5. NOTE: Clearance with INEEL security will have been obtained for all field trip participants prior to leaving the main road; otherwise, this type of activity is prohibited. Drive to the summit for an overview discussion of the silicic domes (Big Southern, Middle, and East Buttes), the ESRP axial vol-

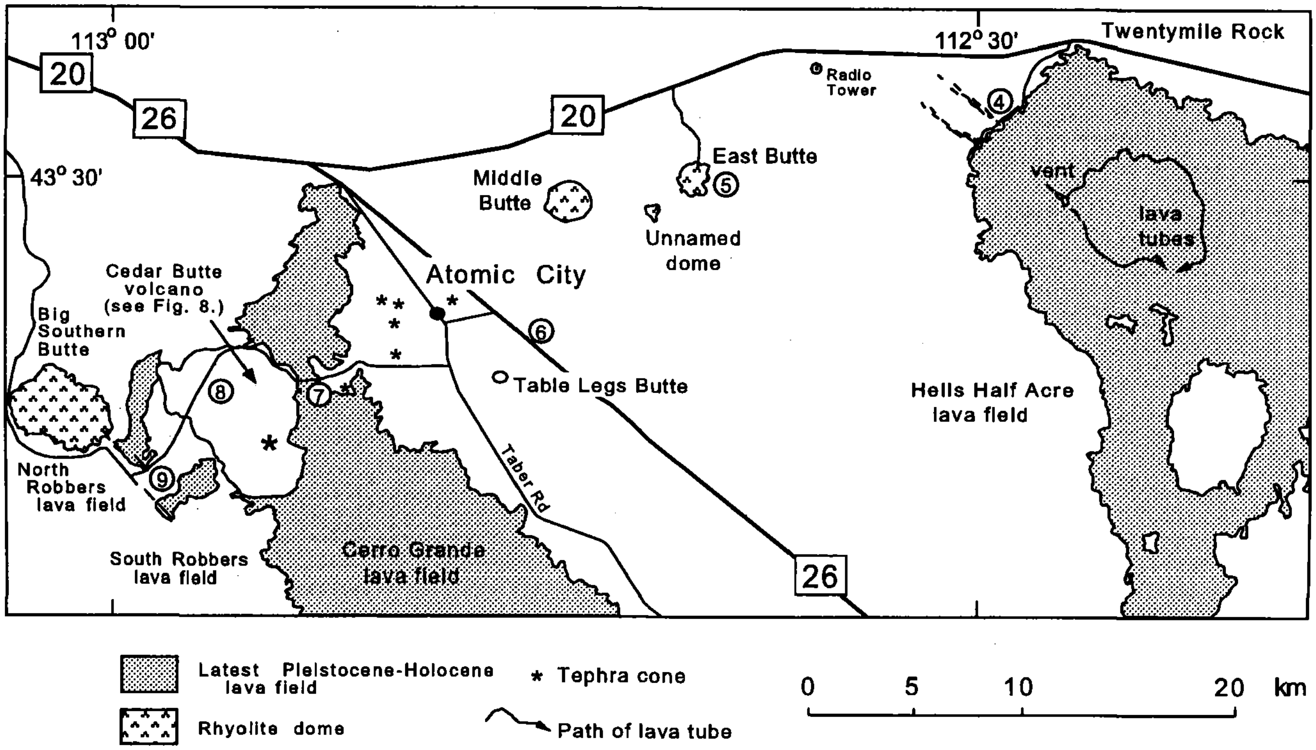

Figure 20. Detailed index map of the eastern Snake River Plain along the axial volcanic zone adapted from Kuntz et al., (1992). Field trip stops are shown in circled numbers. See text for explanation and road guide to Stops 4–9.

canic zone, and hydrogeology of the INEEL (see above sections). A discussion of ESRP range fires and dust storms will also be presented at this stop.

Pleistocene rhyolite domes occur along the axial volcanic zone on the ESRP (Figs. 21, 22). Big Southern Butte is formed of two, coalesced endogenous rhyolite domes (Spear and King, 1982), with an uplifted, north-dipping block of basalts, ferrolatites and sedimentary interbeds on its north flank (Fishel, 1992). The Cedar Butte eruptive center (Spear, 1979; Hayden, 1992) is a complex assemblage of landforms and lava types, mostly intermediate in composition but including a rhyolite lava flow. A topographic escarpment southeast of the Cedar Butte summit may be the result of uplift associated with late-stage silicic-magma intrusion beneath the complex, or the draping of mafic lava flows over a steep-sided silicic flow. Middle Butte is a stack of about twenty basalt lava flows, apparently uplifted in pistonlike fashion by a buried silicic intrusion (cryptodome) of unknown age. East Butte is an endogenous rhyolitic dome, in places containing centimeter-sized clots and blocks of mafic material (Kuntz and Dalrymple, 1979).

Recent range fires on and near the INEEL have provided real-time observations of eolian sediment redistribution processes on the ESRP. Since early 1994, nine range fires have burned over 60,000 acres (95 square miles) of sage and grasslands. Ensuing dust storms whipped up by prevailing winds have caused highway closures and shutdowns of work at some INEEL facilities. Measurements of soil erosion using erosion bridges (Olsen, 1996) and estimates of removed material using height of charred stubble above deflated ground surface indicate that millions to 10's of millions of cubic meters of fine-grained sediments have been mobilized. Very rapid development of new landforms and modification of existing landforms occurred. Within a few days of a 17,000 acre fire in the western part of INEL in 1994, a discontinuous "dune," 20 km long, 1 m high, and several m wide, formed along the eastern (downwind) edge of the fire scar. A 2-m-wide fissure along the east edge of the scar was filled with sediment after the first wind storm.

In the eastern INEEL a 19,000-acre fire in 1996 burned an area that contained a prominent lineament, called the Principal Lineament, which was itself formed by eolian modification of a prehistoric fire scar (Morin-Jansen, 1987). Unique patterns of vegetation, including luxuriant stands of basin wild rye and tall sage, developed on the Principal Lineament because of the relatively coarser sediment with better water holding capacity there. The presence of abundant grasses with good soil-stabilization root systems may preserve the Principal Lineament through this new cycle of

Figure 21. East Butte rhyolite dome at Stop 5 (view from the southwest), one of several Pleistocene silicic volcanic domes on the eastern Snake River Plain axial volcanic zone (see Fig. 14).

burning. Aerial and surface monitoring of the new fire scar as it is revegetated over ensuing years will keep track of the fate of the Principal Lineament and the potential development of new lineaments.

The size, shape, and age variations of numerous historic and prehistoric fire scars on the ESRP, observable on aerial photographs and Landsat images, suggest a continuing process of eolian redistribution of loess following range fires. Implications of the process include: 1. Range fires tend to have the same shapes and sizes in various parts of the plain, reflecting similar prevailing wind directions and fire dynamics. 2. Lineaments are formed and destroyed repeatedly by range-fire and eolian processes. 3. Over the long term, sediment is continually on the move in a down-wind direction. 4. A sorting of the upper few centimeters to decimeters of soil may occur, with fine material being moved farther downwind and coarser material lagging behind. 5. Open fissures in volcanic rift zones may have been filled many times by eolian deposition following range fires and subsequently opened by percolation and piping of water into deeper fracture zones and rubble zones in the volcanic sequence.

6. Table Legs Butte (Scott Hughes)

Drive west on Highway 20, turn southeast on Highway 26 and continue for approximately 9 miles from the junction to milepost 280 for Stop 6. Pleistocene to Holocene basaltic volcanism across the ESRP produced hundreds of small shield volcanoes that have low-angle slopes, cover tens to hundreds of square kilometers, and were built by overlapping pahoehoe lava flows (Hackett and Morgan, 1988). Conveniently located outside the boundary of the INEEL approximately 2.5 miles southeast of Atomic City along highway 26, Table Legs Butte is one of several basaltic shields on the axial volcanic zone not associated with any of the major volcanic rift zones (e.g. Kuntz et al., 1992) that produced spatter ramparts around a prominent summit region. Lavas from this shield are probably 200–400 ka based on geomorphic and stratigraphic relations with other shields (Kuntz et al., 1994); hence most flow surfaces have substantial chaparral vegetation growing in late Pleistocene and Holocene loess-derived soil.

In roadcuts near milepost 280, observe cyclic diktytaxitic texture and vesiculation described above (Fig. 23), and get an overview of the ESRP from the elevated axial volcanic zone. Table Legs basalt in this roadcut contains abundant, up to 40%, phenocrysts of subhedral-to-euhedral plagioclase laths ranging from 0.7 to 1.5 cm in length and less abundant phenocrysts of 1–2 mm olivine. Cyclic layering is evident in phenocryst size and abundance in strongly diktytaxitic shelly pahoehoe (gas rich) lavas erupted from several basaltic shields on the ESRP. Layers range from nearly aphyric to strongly porphyritic with plagioclase laths up to 1 cm comprising over 20 percent of the layer. In some cases, aphyric lava has filled tension fractures developed in plagioclase-phyric lava. Alternating crystal-rich and crystal-poor layers were possibly derived by crystal-liquid segregation during compression and decompression processes within molten cavities that allowed residual liquid to drain out of a crystal network. Crystals are usually intact and either randomly oriented or clustered into star-shaped patterns.

From this point, one can see that Table Legs Butte is a complex shield volcano although evolved compositions similar to those found in Cedar Butte and Craters of the Moon complex eruptive centers have not been found. Aerial photographs indicate that the Table Legs eruptive center is fairly small, approximately 98 km^2, with a ridge of at least 4 eruptive vents on the east flank ~1–2 km from the main vent. These are interpreted as primary vents along a local rift system, the surface expression of dikes, that possibly stopped erupting as volcanism became more concentrated toward the summit region. Smaller vent-like features, mostly squeeze-ups and rootless vents occur on the west and north flanks, some of which are aligned due to breakout along tube-fed flows from the main vent.

7. Cerro Grande lava flow (Scott Hughes and Dick Smith)

Drive 2 miles northwest on Highway 26, turn west on Midway Road leading to Atomic City, and turn south on Taber Road at the south end of Atomic City. Drive 1.3 mi and turn west onto improved unpaved road; continue 4.1 mi to the railroad crossing near the margin of the Cerro Grande lava flow (Stop 7, Fig. 20) and park on the west side of the tracks. Observe flow margin of Cerro Grande lava and the effects of inflationary emplacement of pahoehoe lavas typical of ESRP basalts. The flow margin comprises two parts: a thin outflow "sheet" pahoehoe and an overlying thicker flow made of large inflationary pahoehoe lobes (Fig. 24).

Vesicles and mineral textures reflect variable pressures

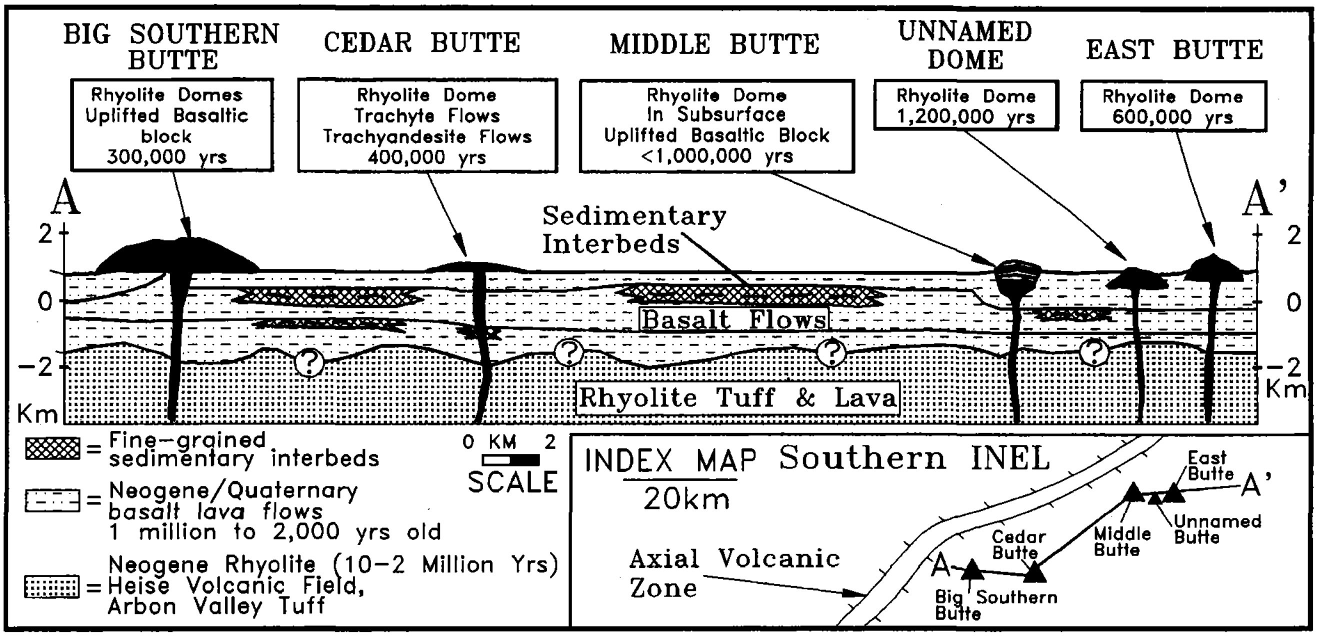

Figure 22. Schematic cross section along the axial volcanic zone of the ESRP, showing the ages, rock types and known or inferred litho-stratigraphic relations of Pleistocene silicic volcanic domes (From p. 146, Link and Phoenix, 1996; modified from Hackett and Smith, 1992).

inside inflating and deflating lava lobes. Layers of vesicles occur in cycles, often as 1–2 cm layers of intensely vesiculated lava separated by 10–20 cm of more massive lava (Fig. 25) representing repeated pressure increase during lobe inflation followed by decompression and volatile exsolution. Thickness of the crust increased with each cycle. The vesicle layers are curved and concentric with lobe surfaces rather than horizontally oriented, due to gravitational rise of bubbles, such as those noted for vesicle layers within Columbia River basalt flows (Manga, 1996). This suggests that molten lava within each lobe experienced cyclic velocity changes as magma repeatedly backed up during marginal cooling then broke out when internal pressure rose above the tensile strength of the crust. Similar processes are noted for sheet flows in Hawaii (Hon et al., 1994)

Climb up the 5–8 m lobe on the northeast side of the tracks where deflationary sagging has resulted in deep tension gashes along the periphery. From this point, one can observe cyclic vesicle layers in the fracture walls related to repeated decompression of the lobe interior as the crust thickened downward. The flow surfaces on the top and flank of the lobe are ropy pahoehoe, typical of the thinner sheet flow on the lower level, that were originally close to horizontal. This observation attests to the significant amount of inflation necessary to produce several meters of uplift due to internal magmatic pressure or gas pressure caused by volatile exsolution.

8. Cedar Butte (Mike McCurry)

Drive west from the railroad crossing on the improved unpaved road for ~2.8 mi, turn south on an unimproved dirt road, and continue ~1.5 mi to where the road splits. Take the left (east) fork and proceed ~0.7 mi to Stop 8 located near the center of Cedar Butte volcano (Figs. 8, 20). Park on the dirt road near a breach in the northern side of the large tephra cone. The purpose of this stop is to discuss possible genetic relationships between evolved mafic-intermediate volcanic centers and high-silica rhyolites of the ESRP. Aspects of the geology and geochemistry of this center are discussed by McCurry et al., above.

Walk north a few tens of meters to the prominent blade-like exposures of mafic dikes. Here you will see three en-echelon dike segments; they are a part of a nearly continuous curvilinear system of vents and intrusions extending for ~2 km, and circumscribing a 150° arc. The arc has a radius of curvature of about 0.8 km, and may have originated by incipient formation of ring fractures above a shallow magma chamber.

These dikes exhibit spectacular features of bimodal magma interaction. The dikes strike N 8° E and dip vertically. The overall dike morphology is wedge-shaped, tapering towards the top, suggesting that the original magma had not propagated to the surface at this location. Contacts with the host tephra are bulbous on a scale of 10's of cm to a meter. Contacts with the host-rock tephra have produced

Figure 23. Cyclic layering of diktytaxitic texture in basalt from Table Legs Butte illustrating relative aphyric and coarsely crystalline horizons (Stop 6). The effect is attributed to successive increase and decrease of pressure within tube-fed lava flows as crust is inflated during magma infilling and then deflated as magma drains through breakout fractures.

a thin zone where the glassy tephra pyroclasts are fused into dense obsidian.

Both southerly dike segments have a layered structure consisting of a core of felsic composition and a rind of more mafic composition (Fig. 26). The interior of the southerly dike is rhyolitic in composition. In the middle segment, the core consists of trachydacite; in both cases the "rind" consists of trachyandesite. Contacts between the two lithologies varies from sharp to gradational over a few centimeters. In many places there are wispy blebs of one lithology within the other. Both features indicate the original magmas were at least partially molten when they were brought into contact. The dike lithologies overlap in composition with the compositions of pyroclasts in the tephra cone to the south, suggesting that the dike is the northern continuation of vents which fed that tephra-cone-forming eruption.

9. North Robbers vent (Dick Smith and Scott Hughes)

Return to the improved unpaved road, continue west ~4.2 mi, and turn right onto a service road. Drive as far as possible, approximately 0.3 mi, to Stop 9 which is located at the vent for the North Robbers lava field (Fig. 20). This is one of the three smallest lava fields (along with South Robbers and Kings Bowl) in the late Pleistocene and Holocene episode of ESRP volcanism. The fissure zone for North Robbers is 2.9 km, and separated into a 1-km-long northern segment, which has both eruptive and non-eruptive components, and a 1.2-km-long southern eruptive segment (Kuntz et al., 1992). The non-eruptive part of the northern segment extends northwest into the Big Southern Butte rhyolite dome. The southern segment is offset from the northern segment and is the primary eruptive fissure system for the North Robbers lava.

Hike up to the summit region which is constructed by a spatter rampart at the vent. This is a good vantage point to observe fairly uncomplicated eruptive features associated with ESRP basalts. On the north side of the cone, the lava channel flow extends north-northeast from the vent area. Walk around to the southeast side to observe the eruptive fissure system oriented northwest-southeast along the Arco volcanic rift zone from which a relatively short lobe of fissure-fed lava flowed northeast.

Return to the vehicles and proceed west on the improved road around Big Southern Butte for ~7 mi to a junction and landing strip on the northwest side of the mountain. Proceed north along the landing strip, stay on the improved road for ~12 mi to Highway 20/26, and continue on to Arco.

10. Craters of the Moon and the Great Rift (Scott Hughes, Bill Hackett and Dick Smith)

Drive southwest from Arco on Highway 20/26 (~18 mi) to Craters of the Moon National Monument and park briefly at the visitor's center for Stop 10A. Covering about 1,600 km^2 with about 30 km^3 of basaltic, and compositionally evolved, lava flows, Craters of the Moon is the largest and most complex of the late Pleistocene and Holocene ESRP basaltic lava fields with eight eruptive periods from 15,000 to 2,100 years ago and quiescent intervals as long as 3000 years (Kuntz, 1989; Kuntz et al., 1982, 1988, 1992). Eruptive vents at are aligned along the northern part of the Great Rift (NW of Kings Bowl and Wapi lava fields in same rift system). Lava flows differ chemically and petrologically from typical SRP olivine tholeiites. Craters of the Moon lavas have olivine tholeiitic parent magmas, but they are fractionated ferrolatites and crustally contaminated. Relative to typical ESRP basalts, their compositions (Fig. 9) exhibit higher Ti, Fe, Na, K, P and lower Mg, Ca.

The Craters of the Moon lava field has nearly every type of feature associated with basaltic systems. Within a few hours time one can observe pahoehoe, a'a, and block lava flows, plus bombs, blocks, scoria and glassy basalt. Spatter cones and cinder cones with widely ranging tephra size fractions reflect variable viscosity and eruptive mechanisms. Vent alignments along fissures and evidence for multiple eruptive phases from the larger craters are evident. Lava flows exhibit squeeze-ups, pressure ridges, lava tubes, levees, hornitos, driblet cones and spires, lava stalactites, tumuli, kipukas, extension cracks, scarps, rafted blocks, and tree molds. Please note that off-trail hiking is allowed anywhere in Craters of the Moon National Monument *except* for the spatter cones area and the North Crater Flow,

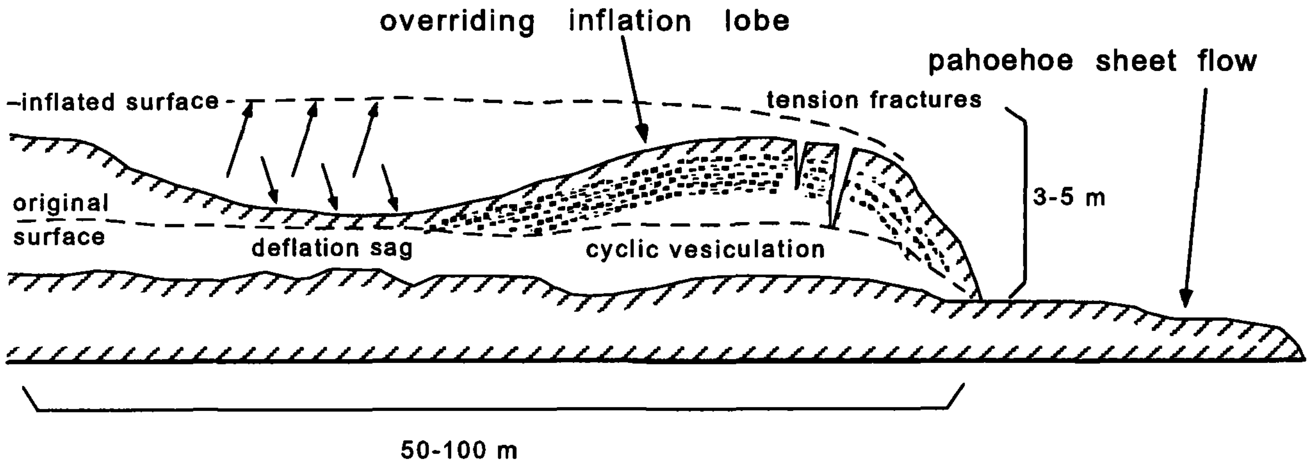

Figure 24. Schematic diagram of thick pahoehoe lobe over thinner sheet-like pahoehoe flow observed in the Cerro Grande basalt at Stop 7. Cyclic vesiculation, tension fractures, and sagging are related to repeated pressure fluctuations as magma inflates and deflates the lobe as the solid crust becomes thicker with cooling.

but that absolutely NO sampling is allowed anywhere in the monument.

After a brief stop in the visitor center follow the park road (Fig. 27) across North Crater Flow (note large rafted blocks of agglutinated tephra), around North Crater and Paisley Cone, between Big Craters and Inferno Cone to the Spatter Cones parking area. This is Stop 10B, where three small spatter cones (one with perpetual snow and ice in the crater) are aligned with Big Craters cinder cone complex along a fissure. Walk ~50 m over to the closest spatter cone to observe the plastically-deformed agglutinate in a high angle of repose. Inside the cone one can observe drainback features and the highest level of lava rise during the eruptive phase. Hike ~100 m northwest along the trail up to the rim of Big Crater and note the tephra stratification sequence on the opposite wall and nested eruptive pits in the floor. At least three eruptive phases are evident from the rim at this location; more can be seen on a brief walk around the rim. Facing south, one can observe the Blue Dragon lava flows, the youngest in the lava field (Kuntz et al., 1988), which exhibit the characteristic smooth pahoehoe surface sheen punctuated by rough zones of a'a lava.

Continue southeast on the park road (Fig. 27) between the Inferno Cone and Blue Dragon lavas, then to lava tubes in the Blue Dragon flows (Stop 10C) and prepare for hiking in cool dark lava tubes. Follow the marked paved trail eastward ~0.5 km to Indian Tunnel, a lava tube with several collapsed roof sections that allow hiking without artificial illumination. While hiking through this cave (~100 m) observe the walls and floor and note various lava levels, stalactites and drainouts from alcoves that occurred when the tube was emptied. In particular, notice the floor in places where ceiling blocks have not obscured the original texture of the flow surface. The cooling rate was obviously much higher inside the tube so the floor is not glassy-smooth like the outside surfaces. Instead, a cm-scale roughness is evident that was likely caused by stretching and buckling while the surface cooled much slower than the flow surface outside the tube. Other caves may be visited before continuing on the next stop.

Leave the caves area and continue around the northeast side of Inferno Cone and east side of Paisley Cone to Devils Orchard. At this point observe the rough block and a'a flows that formed from higher-viscosity latite lava. This flow probably erupted from North Crater (Kuntz, 1989); it has steep 5-m flow fronts and 20-m-high rafted blocks of bedded cinders derived from the cone. Leave the monument through the front entrance and drive northeast on Highway 20/26 back to Arco. This is the final stop of the second day.

Day Three

11. Box Canyon (Dick Smith and Bill Hackett)

Box Canyon Graben

Drive southeast from Arco on Highway 20/26 ~1.3 mi to an intersection on the right with two improved unpaved roads, one bearing south and the other bearing west. Drive ~1.1 mi south and southeast to an intersection, continue on the south (right) branch 2.2 mi, across the bridge over Big Lost River, to an intersection where the "main" road (left branch) continues southeast. Follow this road 1.4 mi, then turn northeast (left) and go ~0.8 mi to where the road takes several bends near the edge of Big Lost River and

Figure 25. Cyclic vesiculation in Cerro Grande lava observed at Stop 7.

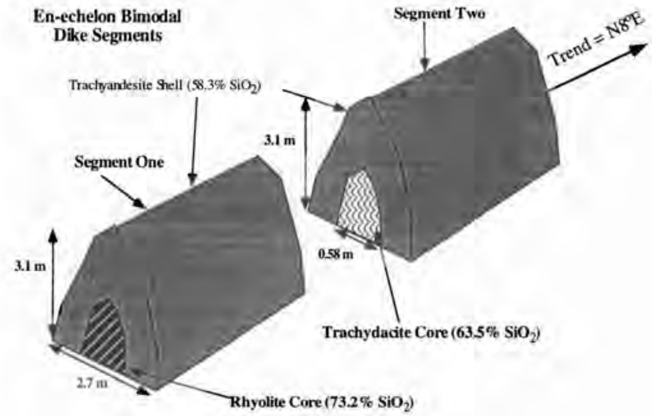

Figure 26. Schematic diagram of segmented en-echelon bimodal dike observed at Stop 8. The basaltic dike is cored by compositionally evolved trachydacite and rhyolite.

drops down in elevation for Stop 11A (Fig. 28). Upstream (northwest) from this point, the river flows within and parallel to the Arco volcanic rift zone (Fig. 14). Downstream, it flows northeast, then back southeast along the rift trend cutting into ESRP basalts forming Box Canyon.

This stop is on the southwest margin of the Box Canyon graben, a linear NW-SE topographic depression that controls the Big Lost River and marks the northern extent of dike-induced structures in the Arco volcanic rift zone. From this point and southeastward to Big Southern Butte, Arco volcanic rift zone surface deformation features and vents (Smith et al., 1989, 1996; Hackett and Smith, 1992) are typical of those observed in volcanic rift zones in Iceland and Hawaii (Pollard et al., 1983; Rubin and Pollard, 1988; Rubin, 1992). Fissures, fissure swarms, small normal faults, graben, eruptive fissures, and monogenetic shield volcanoes are abundant in this zone. From this point northwestward to the town of Arco, the origin of structures is ambiguous and transitional to the Lost River fault, which is well developed north of Arco. The identification of late Quaternary fault scarps on the Lost River fault is clear and unequivocal from Arco to the north, but terraces along the Big Lost River and Holocene incision and deposition along a small drainage that joins the Big Lost River just south of Arco obscure any possible fault scarps and make identification of the fault uncertain (Scott, 1982). Reflection seismic surveys show displacements attributable to the Lost River fault for a distance of about 5 or 6 km south of Arco, but none in the area of the Box Canyon graben. Because of the uncertainty in fault identification, and the distance of possible epicenters of earthquakes to INEEL facilities is sensitive to the position of the southern end of the Lost River fault, several scenarios for the southern termination are used in seismic hazards assessment.

The Box Canyon graben probably represents the cumulative effects of several dike intrusion events into this part of the volcanic rift zone. The tilting of slabs of basalt and the fan-like separation of columnar joint blocks, typical of deformation due to dike intrusion in volcanic rift zones worldwide, is visible here in the area where the river cuts into the northeast limb of the graben. Figure 6 shows the relationship of volcanic rift zone graben to dikes in the shallow subsurface.

Glacial Outburst Flooding.

Drive southeast from Stop 11A for ~0.1 mi to a fork, continue on the left branch 1.8 mi to a junction and take the left branch, which is the main road travelled before turning off to the last stop (Fig. 28). Drive 1.3 mi southeast, take the left fork, continue another 1.0 mi and turn northeast (left) onto a service road for 0.2 mi which leads to a well for Stop 11B. This stop is in the Arco volcanic rift zone just to the southeast of the Box Canyon graben where clear evidence for a late Pleistocene glacial outburst flood(s) exists (Rathburn, 1991, 1993). After an overview of glacial flooding, observe the erosional loess scarp and walk around on basalt stripped bare of soil. Erosional features caused by the flooding include cataracts in basaltic terrain, scabland topography, and scouring of loess from the basalt lavas, leaving a scarp that marks the edge of the flood. The loess scarp and scoured basalt surface can be recognized on landsat images of the area. Depositional features include boulder bars and ice-rafted erratic boulders. Flood discharge was 60,000 cubic meters per second. The age of flooding was about 20,000 years B.P., near the time when several

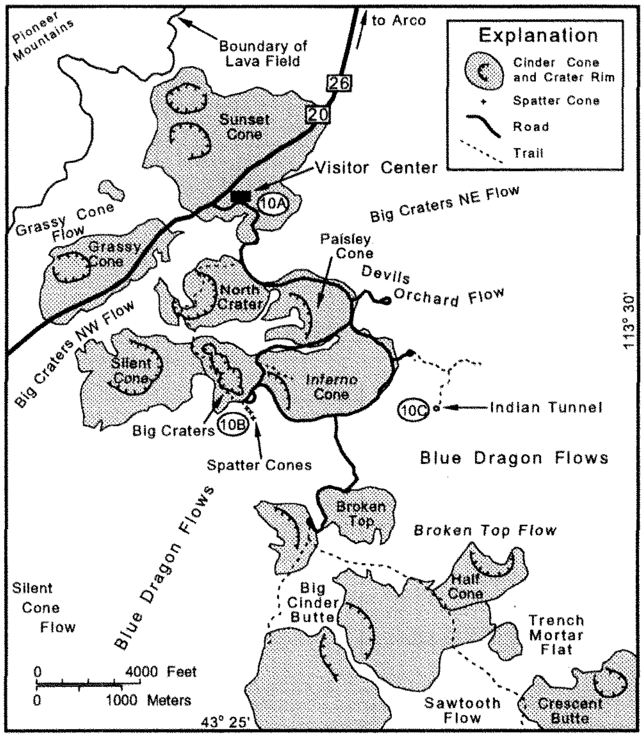

Figure 27. Index map of the Craters of the Moon National Monument area (adapted from Kuntz, 1989) showing tephra cones and general locations of major lava flows. Field trip Stops 10A–10C are only a few of the numerous places in the monument where fresh volcanic features can be observed.

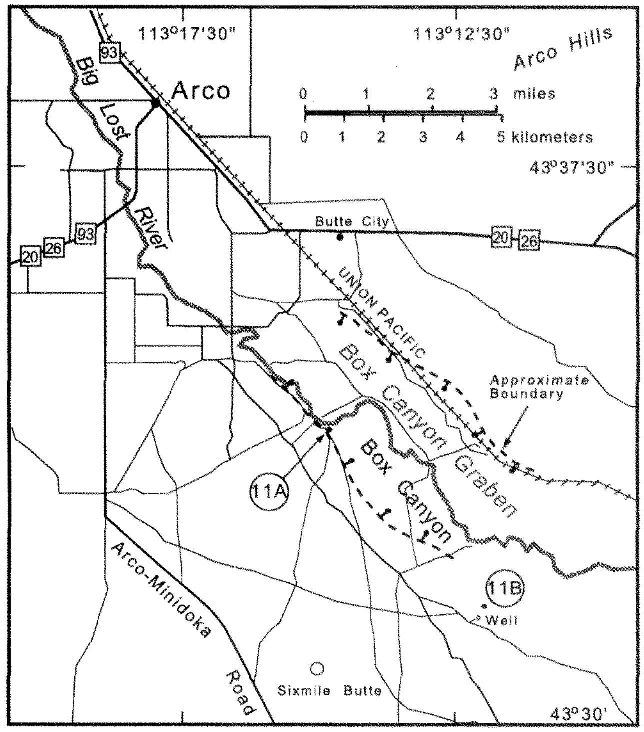

Figure 28. Map of unimproved roads (thin solid lines) south of Arco, Idaho illustrating access to Box Canyon graben. The Big Lost River flows southeast in a direction structurally controlled by the Arco volcanic rift zone (see Fig. 14). Stop 11A will allow observation of Box Canyon graben, which follows the same structural trend. Geomorphic features related to catastrophic glacial flooding are observed at Stop 11B. See text for explanation and road guide from Arco.

other glacial outburst flooding episodes occurred in the western U.S., and may mark the beginning of glacial melting after the last glacial maximum (Cerling et al., 1994).

Drive 0.2 mi back to the road and turn northwest (right); continue 0.4 mi to an intersection and follow the west (left) branch ~2.6 mi to a crossroads. Sixmile Butte, an ESRP basaltic shield volcano, can be observed off to the south. Turn south (left), drive 1.9 mi to the Arco-Minidoka Road (Fig. 28), and continue driving south ~19 mi to the junction of an improved unpaved road that branches eastward to Coxs Well. Remain on the Arco-Minidoka Road and mark mileage.

12. Kings Bowl Lava Field (Scott Hughes and Dick Smith)

Drive south on the Arco-Minidoka Road ~23 mi past Coxs Well junction to the intersection with the road to Crystal Ice Cave (Fig. 29). This intersection is reached 0.2 mi *before* reaching Bear Trap Cave, a lava tube with a large (~30 m) entrance on the right side of the road. Travel southeast ~2.4 mi to a junction, turn left (east) and proceed ~8 mi. to the Kings Bowl lava field for Stop 12. Park in the area once reserved for public visitors (the visitor's center is abandoned now) on the northeast side of the rift and walk northwest along the fissure system to gain access to the opposite side. For an extended field trip, Greeley et al., (1977) provide an excellent and much detailed guide to this lava field.

The Kings Bowl lava field is the smallest of three eruptive centers (besides Wapi and COM) on the Great Rift, yet it provides an ideal place to observe many features related to a fissure eruption that culminated in a phreatic phase. The final explosion ejected blocks of chilled Kings Bowl lava and older flows up to several meters created a pit that is 85 m long, 30 m wide and 30 m deep. Many of the ejected blocks broke through the lava crust while the interior was still molten. Radiocarbon dating of this eruption (Kuntz et al., 1986b) indicates an age of 2,222 ± 100 years B.P., and Kuntz (1992) suggests that the field represents a single burst of activity over a period as little as six hours. Kings Bowl (a phreatic explosion pit) and Crystal Ice Cave (a section of the fissure system) have been visited

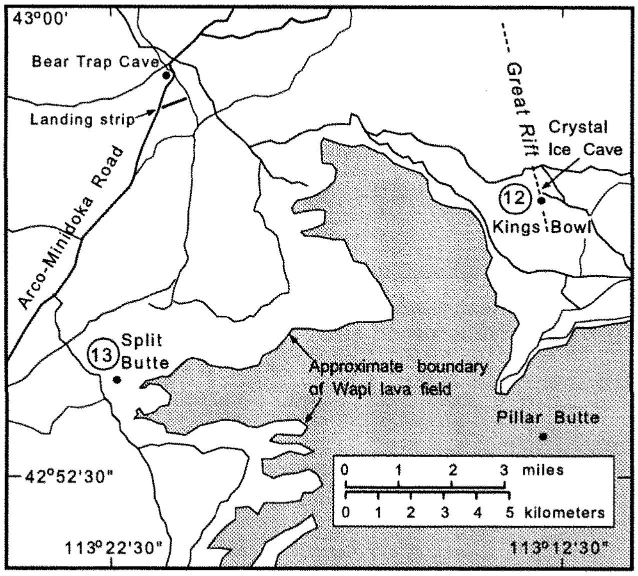

Figure 29. Index map of the Kings Bowl (Stop 12) and Split Butte (Stop 13) areas showing access roads (thin solid lines) and the approximate boundary of the Holocene Wapi lava field. Crystal Ice Cave and Kings Bowl have been popular attractions to tourists and adventurers for many years. See Greeley et al., (1977) for detailed map.

extensively by the public and received much attention in geologic studies (e.g. Greeley et al., 1977; Kuntz et al., 1982, 1992). Fissure-fed lava issued from numerous points along a 6.2-km-long en-echelon fracture system (Fig.30). Two sets of non-eruptive fractures approximately 1.5 km apart occur on opposite sides of and parallel to the central eruptive fissures. They are associated with dike injection and easily recognized from aerial photographs and at ground level.

There are many places along the rift and on the lava field that are potentially dangerous to hikers and climbers, so be alert when working in this area. The northeast side of the field is covered with tephra blown downwind during the phreatic phase; however, numerous ejecta blocks can be found on both sides (except near Kings Bowl where vandals pushed most of the blocks into the pit). The lava field is relatively flat compared to most ESRP flows and constituted several shallow coalescent and terraced lava lakes of shelly pahoehoe representing compound lava flows. There are several places on the field where lava drained back into the fissure, merged with other flows, or forced slabs of hardened crust upward.

On the lava lake, observe the crust where it was broken while the interior was still molten. Stacks of lava crust slabs forming mounds are possibly remnants of a levee. Some cracks resulted in elongate lava squeeze-ups although circular dome-like squeeze-ups become more apparent closer to the phreatic pit. These were produced when ejecta blocks broke through the lava lake, often resulting in radial fractures, and allowed molten gassed-charged lava to ooze out forming a blister of quenched lava on the surface. Some ejecta blocks can still be observed encased in the hollow protuberances.

Enter the phreatic pit from the northeast side where a walkway has been established and note the layers of fresh Kings Bowl lava covering baked soils, tephra, and underlying older ESRP lava flows. The lower surfaces of individual lava lobes exhibit festoon-like swirls and bulges, attributed to low viscosity flow, where they covered freshly-chilled crusts of previous lobes. The feeder dike for the eruption can be seen at the north end of the pit where it is chilled against earlier flows. Vesicle pipes and vesicular zones extending upwards from the base of the flow suggest volatile entrainment, possibly from a moist subsurface.

The Wapi lava field, composed of many thin overlapping pahoehoe flows (Champion, 1973; Champion and Greeley, 1977), lies ~4 km south of the Kings Bowl lava field. The Wapi vents do not lie on an extension of the Kings Bowl fissures; however, a radiocarbon age of 2,270 ± 50 B.P. (Champion and Greeley, 1977; Kuntz et al., 1986b) for the Wapi system suggests that, within analytical uncertainty, the two centers are contemporaneous. Thus, the three lava fields associated with the Great Rift exhibit the highest Holocene activity of the ESRP basaltic rift systems.

13. Split Butte (Scott Hughes)

Drive west back to the Minidoka-Arco Road and turn south; proceeding 0.2 mi to Bear Trap Cave, a segment of a 21 km long lava tube that is an alternate stop if time permits. Continue south toward Minidoka approximately 4.5 mi., turn left off main road, toward Split Butte (Fig. 29). Drive along the access road toward the low point on the west rim of the crater and, where the break in slope prohibits driving further, continue on foot to the rim for Stop 13. Walk along the rim to observe tephra sequences then down the inner slope to the edge of the basalt cliff.

Located about one km west of the Wapi lava field, Split Butte is a maar type phreatomagmatic crater (Fig. 31) that is one of the older exposed features on the ESRP (Womer, 1977; Womer et al., 1982). It consists of a subcircular tephra ring ~0.6 km in diameter with an inner basalt lava lake, which suggests that an initial eruptive phase caused by basaltic magma interacting with groundwater was followed by an effusive phase. The inner lava lake rose to a depth within the ring that was higher than the surrounding lava surface then, after minor overflow on the southwest flank, it subsided to leave a circular terrace-like platform around the inside margin of the crater. The tephra ring is surrounded by loess-covered Quaternary ESRP basalts. The

Figure 30. Segment of the fissure system at the Holocene Kings Bowl lava field located along the Great Rift volcanic rift zone on the eastern Snake River Plain.

Holocene Wapi flows stopped short of lapping up on the southeast flank. The lava lake effusive eruption was probably fairly quiet, as indicated by a lack of spatter, although slumping within the tephra ring resulted in a disconformable contact visible between it and the surrounding basalt lava.

Womer et al., (1982) point out several lines of evidence for a phreatomagmatic origin. The ash is mostly clear palagonitized sideromelane that is typically blocky and angular with few vesicles, indicating rapid quenching in a wet environment. Plastic deformation of ash layers also occurs beneath ejecta blocks, and secondary minerals such as calcite and zeolite are abundant. Pyroclastics typical of strombolian eruptions are generally absent and layers of hyaloclastite-rich coarse tephra are interspersed with fine ash having accretionary lapilli.

This is the final stop of the field trip. Drive back to the Arco-Minidoka Road, continue ~10 mi south to Minidoka and take Route 24 ~17 mi southwest to the I-84 freeway.

Figure 31. Split Butte (looking northwest), a phreatomagmatic maar-type volcano comprised of a tephra ring and inner basalt lava lake. The lava lake partially flowed over the southwest rim and collapsed leaving a circular shelf of basalt within the crater.

ACKNOWLEDGEMENTS

The authors benefited from discussions, fields excursions and unselfish sharing of ideas with geologists who have worked on eastern Snake River Plain basaltic systems over the past two decades. We are especially indebted to Ron Greeley, Arizona State University; Mel Kuntz and Duane Champion, U.S. Geological Survey; Bill Leeman, Rice University; Dave Rodgers, Idaho State University; and the numerous coworkers of these individuals. Technical reviews by Mel Kuntz, Dennis Geist, Ron Greeley, and Paul Link are greatly appreciated and significantly improved the quality of the manuscript. Much of the work reported in this guide was supported by the U.S. Department of Energy, Office of New Production Reactors and Assistant Secretary for Environmental Management, under DOE Idaho Operations Office Contract DE-AC07-94ID13223. Additional support was provided by grant #DE-FG07-96ID13420 from the U.S. Department of Energy to the Idaho Water Resources Research Institute, subcontract #KEK066-97-B to Idaho State University; and various Task Orders under EG&G, Idaho Contract C84-110421 to M. McCurry and S. Hughes.

REFERENCES CITED

Alt, D, Sears, J M, and Hyndman, D.W., 1988, Terrestrial maria. The origins of large basalt plateaus, hotspot tracks and spreading ridges. Journal of Geology, v. 96, p. 647–662.

Anders, E., and Ebihara, M., 1982, Solar-system abundances of the elements. Geochimica et Cosmochimica Acta, v. 46, p 2360–2380

Anders, M.H. and Sleep, N.H, 1992, Magmatism and extension: The thermal and mechanical effects of the Yellowstone hotspot Jour Geophysical Res., v. 97, p. 15,379–15,393.

Anders, M.H., Geissman, J.W., Piety, L.A., and Sullivan, J T, 1989, Parabolic distribution of circum-eastern Snake River Plain seismicity and latest Quaternary faulting. migratory pattern and association with the Yellowstone hot spot· Jour Geophysical Res., v. 94, n B2, p. 1589–1621.

Anderson, S R., and Bartholomay, R.C., 1995, Use of natural gamma logs and cores for determining stratigraphic relations of basalt and sediment at the Radioactive Waste Management Complex, Idaho National Engineering Laboratory, Idaho Journal of the Idaho Academy of Science, v. 31, no. 1, p. 1–10.

Anderson, S R, Ackerman, D.J., Liszewski, M.J., and Feiburger, R.M, 1996, Stratigraphic data for wells at and near the Idaho National Engineering Laboratory, Idaho. U.S. Geological Survey Open-File Report 96-248 (DOE/ID-22127), 27 p. and 1 diskette.

Armstrong, R.L., Leeman, W.P., and Malde, H.E., 1975, K-Ar dating, Quaternary and Neogene volcanic rocks of the Snake River Plain, Idaho: American Journal of Science, v 275, p. 225–251.

Barraclough, J.T., and Jensen, R.G., 1976, Hydrologic data for the Idaho National Engineering Laboratory site, Idaho, 1971 to 1973 U S. Geological Survey Open-File Report 75-526 (IDO-22060), p 116.

Bartholomay, R.C., Orr, B R, Liszewski, M.J., and Jensen, R G., 1995, Hydrologic conditions and distribution of selected radiochemical and chemical constituents in water, Snake River Plain aquifer, Idaho National Engineering Laboratory, Idaho, 1989 through 1991: U.S. Geological Survey Water-Resources Investigations Report, 95-4175 (DOE/ID-22123), 47 p.

Bergantz, G.W, and Dawes, R., 1994, Aspects of magma generation and ascent in continental lithosphere, *in* Ryan, M.P., ed., Magmatic Systems, Academic Press, New York, p. 291–317.

Bryan, W.B., Finger, L W., and Chayes, F., 1968, Estimating proportions in petrographic mixing equations by least-squares approximation Science, v. 163, p. 926–927.

Carr, W.J., and Trimble, D.E., 1963, Geology of the American Falls Quadrangle, Idaho. U.S. Geological Survey Bulletin, 1121-G, 43 p

Cecil, L.D., Orr, B.R., Norton, T., and Anderson, S R, 1991, Formation of perched groundwater zones and concentrations of selected chemical constituents in water, Idaho National Engineering Laboratory, Idaho 1986–88 U S. Geological Survey Water-Resources Investigations Report 91-4166 (DOE/ID-22100), 53 p.

Cerling, T.E., Poreda, R.J., and Rathburn, S.L., 1994, Cosmogenic ^{3}He and ^{21}Ne age of the Big Lost River flood, Snake River Plain, Idaho: Geology, v.22, p.227–230.

Champion, D.E., 1973, The relationship of large scale surface morphology to lava flow direction, Wapi lava field, SE Idaho [M S thesis]. Buffalo, State University of New York at Buffalo, 44 p.

Champion, D E, and Greeley, R., 1977, Geology of the Wapi lava field, Snake River Plain, Idaho, *in* Greeley, R, and King, J.S., eds., Volcanism of the eastern Snake River Plain, Idaho: A Comparative planetary guidebook Washington, D.C., National Aeronautics and Space Administration, p 135–151.

Christiansen, R.L., and McKee, E.H., 1978, Late Cenozoic volcanic and tectonic evolution of the Great Basin and Columbia intermontane regions. Geological Society of America Memoir 152, p 283–311

Creighton, D.N., 1982, The geology of the Menan complex, a group of phreatomagmatic constructs in the eastern Snake River Plain, Idaho [M.S. thesis]: Buffalo, State University of New York at Buffalo, 76 p.

Creighton, D N, 1987, Menan Buttes, southeastern Idaho, *in* Beus, S S, ed, Centennial field guide volume 2, Rocky Mountain Section of the Geological Society of America, p. 109–111

Eaton, G P, and 7 others, 1975, Magma beneath Yellowstone National Park. Science, v 188, p 787–796.

Embree, G.F., McBroome, L.A., and Doherty, D J., Preliminary stratigraphic framework of the Pliocene and Miocene rhyolite, eastern Snake River Plain, Idaho; *in* Bonnichsen, Bill, and Breckenridge, R.M., eds., Cenozoic Geology of Idaho Idaho Bureau of Mines and Geology Bulletin 26, p. 333–344.

Ferdock, G.C., 1987, Geology of the Menan volcanic complex and related features, northeastern Snake River Plain, Idaho [M.S. thesis]: Pocatello, Idaho State University, 171 p

Fishel, M.L., 1993, The geology of uplifted rocks on Big Southern Butte. Implications for the stratigraphy and geochemistry of the Eastern Snake River Plain [M.S thesis]: Pocatello, Idaho State University, 178 p.

Fleck, R.J., and Criss, R E, 1985, Strontium and oxygen isotopic variations in Mesozoic and Tertiary plutons of central Idaho Contributions to Mineralogy and Petrology, v. 90, p 291–308.

Frederick, D.B., and Johnson, G S, 1996, Estimation of hydraulic properties and development of a layered conceptual model of the Snake River Plain aquifer at the Idaho National Engineering Laboratory, Idaho: State of Idaho INEL Oversight Program and Idaho Water Resources Research Institute, Technical Completion Report, 67 p and appendices

Geist, D., and Richards, M., 1993, Origin of the Columbia Plateau and Snake River plain. Deflection of the Yellowstone plume Geology, v 21, p. 789–792.

Geslin, J.K., Gianniny, G L., Link, P.K., and Riesterer, J.W., 1997, Subsurface sedimentary facies and Pleistocene stratigraphy of the northern Idaho National Engineering and Environmental Laboratory. Controls on hydrology; *in* Sharma, S., and Hardcastle, J H., eds, Proceedings of the 32nd Symposium on Engineering Geology and Geotechnical Engineering, p. 15–28

Gianniny, G.L., Geslin, J K, Riesterer, J., Link, P.K., and Thackray, G.D., 1997, Quaternary surficial sediments near Test Area North (TAN), northeastern Snake River Plain: An actualistic guide to aquifer characterization; *in* Sharma, S, and Hardcastle, J.H., eds., Proceedings of the 32nd Symposium on Engineering Geology and Geotechnical Engineering, p. 29–44.

Greeley, R., 1977, Basaltic "plains" volcanism, *in* Greeley, R, and King, J.S., eds., Volcanism of the eastern Snake River Plain, Idaho. A Comparative planetary guidebook: Washington, D.C., National Aeronautics and Space Administration, p. 23–44.

Greeley, R, 1982, The Snake River Plain, Idaho: Representative of a new category of volcanism Journal of Geophysical Research, v 87, p. 2705–2712.

Greeley, R, and King, J.S., 1977, eds., Volcanism of the eastern Snake River Plain, Idaho· A Comparative planetary guidebook: Washington, D.C., National Aeronautics and Space Administration, 308 p

Greeley, R., Theilig, E., and King, J.S., 1977, Guide to the geology of Kings Bowl lava field, *in* Greeley, R., and King, J.S., eds., Volcanism of the eastern Snake River Plain, Idaho: A comparative planetary guidebook: Washington, D C., National Aeronautics and Space Administration, p 171–188.

Hackett, W.R., and Morgan, L.A., 1988, Explosive basaltic and rhyolitic volcanism of the eastern Snake River Plain; *in* Link, P.K., and Hackett, W R., eds., Guidebook to the Geology of Central and Southern Idaho: Idaho Geological Survey Bulletin 27, p. 283–301

Hackett, W.R., and Smith, R.P., 1992, Quaternary volcanism, tectonics, and sedimentation in the Idaho National Engineering Laboratory area, *in* Wilson, J.R., ed., Field Guide to Geologic Excursions in Utah and Adjacent areas of Nevada, Idaho, and Wyoming. Utah Geological Survey, Miscellaneous Publication 92-3, p. 1–18.

Hackett, W.R., and Smith, R.P., 1994, Volcanic hazards of the Idaho National Engineering Laboratory and adjacent areas. U.S. Department of Energy, Idaho National Engineering Laboratory Document INEL-94/0276, 31 p

Hamilton, W.B., 1989, Crustal geologic processes of the United States; *in* Pakiser, L.C., and Mooney, W.D., Geophysical framework of the continental United States. Geological Society of America Memoir 172, p. 743–781.

Hayden, K.P., 1992, The geology and petrology of Cedar Butte, Bingham County, Idaho [M.S. thesis]. Pocatello, Idaho State University, 104 p

Hayden, K.P., McCurry, M., Hackett, W.R, and Mertzman, S.A, 1992, Geology and petrology of Cedar Butte Volcano, Eastern Snake River Plain, Idaho. Geological Society of America Abstracts with Programs, 24, p. 6.

Hildreth, W., Halliday, A.N., and Christiansen, R L., 1991, Genesis and contamination of basaltic and rhyolitic magma beneath the Yellowstone Plateau volcanic field: Journal of Petrology, v. 32, p 63–138.

Hon, K., Kauahihaua, J, Denlinger, R, and McKay, K, 1994, Emplacement and inflation of pahoehoe sheet flows. observations and measurements of active lava flows on Kilauea Volcano, Hawaii: Geological Society of America Bulletin, v. 106, p. 351–370.

Hughes, S.S., Casper, J.L., and Geist, D.J., 1997, Potential influence of volcanic constructs on hydrogeology beneath Test Area North, Idaho National Engineering and Environmental Laboratory, Idaho; *in* Sharma, S, and Hardcastle, J.H., eds., Proceedings of the 32nd Symposium on Engineering Geology and Geotechnical Engineering, p. 59–74.

Jakobsson, S.P., and Moore, J.G., 1982, The Surtsey research drilling project of 1979. Surtsey Research Report, v. 9, p. 76–93.

Jakobsson, S P., and Moore, J G., 1986, Hydrothermal minerals and alteration rates at Surtsey volcano, Iceland: Geological Society of America Bulletin, v. 97, p. 648–659

Keszthelyi, L, and Denlinger, R., 1996, The initial cooling of pahoehoe flow lobes. Bulletin of Volcanology, v. 58, p. 5–18.

Knobel, L.L., Cecil, L D, and Wood, T R., 1995, Chemical composition of selected core samples, Idaho National Engineering Laboratory, Idaho. U.S. Geological Survey Open-File Report 95-748, 59 p

Kuntz, M.A., 1979, Geologic map of the Juniper Buttes area, eastern Snake River Plain, Idaho. U.S. Geological Survey Miscellaneous Investigations Series, Map I-1115, 1.48,000.

Kuntz, M A, 1989, Geology of the Craters of the Moon Lava Field, Idaho Field Trip Guidebook T305, American Geophysical Union, p. 51–61.

Kuntz, M.A., 1992, A model-based perspective of basaltic volcanism, eastern Snake River Plain, Idaho, *in* Link, P.K., Kuntz, M A, and Platt, L.P, eds., Regional geology of eastern Idaho and western Wyoming Geological Society of America Memoir 179, p. 289–304.

Kuntz, M A., and Kork, J O., 1978, Geology of the Arco-Big Southern Butte area, eastern Snake River Plain, and potential volcanic hazards to the Radioactive Waste Management Complex, and other waste storage and reactor facilities at the Idaho National Engineering Laboratory, Idaho: U S Geological Suvey Open-File Report 78-691, p. 70.

Kuntz, M.A., and Dalrymple, G.B., 1979, Geology, geochronology, and potential volcanic hazards in the Lava Ridge-Hell's Half Acre area, eastern Snake River Plain, Idaho, U.S. Geological Survey Open-File Report 79-1657, p. 70.

Kuntz, M.A., Dalrymple, G.B., Champion, D.E., and Doherty, D.J., 1980, Petrography, age, and paleomagnetism of volcanic rocks at Radioactive Waste Management Complex, Idaho National Engineering Laboratory, Idaho, with an evaluation of volcanic hazards. U.S. Geological Survey Open File Report 80-388, 63 p.

Kuntz, M.A, Champion, D E, Spiker, E.C., Lefebvre, R.H, and McBroome, L.A., 1982, The Great Rift and the evolution of the Craters of the Moon lava field, Idaho, *in* Bonnichsen, Bill, and Breckenridge, R M., eds., Cenozoic Geology of Idaho Idaho Bureau of Mines and Geology Bulletin 26, p. 423–438

Kuntz, M.A., Champion, D.E., Spiker, E C, and Lefebvre, R.H., 1986a, Contrasting magma types and steady-state, volume-predictable volcanism along the Great Rift, Idaho: Geological Society of America Bulletin, v 97, p. 579–594.

Kuntz, M.A., Spiker, E C, Rubin, M., Champion, D E., Lefebvre, R.H., 1986b, Radiocarbon studies of latest Pleistocene and Holocene lava flows of the Snake River Plain, Idaho, data, lessons, interpretations: Quaternary Research, v. 25, p. 163–176.

Kuntz, M.A., Champion, D E, Lefebvre, R H, and Covington, H R, 1988, Geologic map of the Craters of the Moon, Kings Bowl, Wapi lava fields and the Great Rift volcanic rift zone, south-central Idaho: U S. Geological Survey Miscellaneous Investigation Series Map I-1632, scale 1.100,000.

Kuntz, M A., Covington, H R, and Schorr, L J, 1992, An overview of basaltic volcanism of the eastern Snake River Plain, Idaho, *in* Link, P.K., Kuntz, M.A., and Platt, L.P., eds, Regional geology of eastern Idaho and western Wyoming: Geological Society of America Memoir 179, p. 227–267

Kuntz, M.A., Skipp, B, Lanphere, M.A., Scott, W.E, Pierce, K.L., Dalrymple, G.B., Champion, D.E., Embree, G F, Page, W R., Morgan, L A, Smith, R.P., Hackett, W.R., and Rodgers, D.W., 1994, Geologic map of the Idaho National Engineering Laboratory and adjoining areas, eastern Idaho. U.S. Geological Survey Miscellaneous Investigations Series Map 1-2330, scale 1:100,000.

Lanphere, M.A., Kuntz, M A, and Champion, D.E., 1994, Petrography, age, and paleomagnetism of basaltic lava flows in coreholes at Test Area North (TAN), Idaho National Engineering Laboratory, U.S. Geological Survey Open-File Report 94-686, 49 p

Le Bas, M.J., Le Maitre, R.W., Streckeisen, A., and Zanettin, B., 1986, A chemical classification of volcanic rocks based on the total alkali-silica diagram, Journal of Petrology, v 27, p. 745-750

Leeman, W.P, 1982a, Development of the Snake River Plain—Yellowstone Plateau province, Idaho and Wyoming. An overview and petrologic model, *in* Bonnichsen, Bill, and Breckenridge, R M, eds., Cenozoic Geology of Idaho, Idaho Bureau of Mines and Geology Bulletin 26, p. 155–177.

Leeman, W.P., 1982b, Evolved and hybrid lavas from the Snake River Plain, Idaho; *in* Bonnichsen, Bill, and Breckenridge, R.M., eds., Cenozoic Geology of Idaho, Idaho Bureau of Mines and Geology Bulletin 26, p. 193–202.

Leeman, W.P., 1982c, Rhyolites of the Snake River Plain-Yellowstone Plateau province, Idaho and Wyoming. A summary of petrogenetic models; *in* Bonnichsen, Bill, and Breckenridge, R.M., eds., Cenozoic Geology of Idaho, Idaho Bureau of Mines and Geology Bulletin 26, p. 203–212.

Leeman, W.P., Vitaliano, C.J., and Prinz, M., 1976, Evolved lavas from the Snake River Plain, Craters of the Moon National Monument, Idaho Contributions to Mineralogy and Petrology, v. 56, p. 35–60

Leeman, W P, Menzies, M A , Matty, D J., and Embree, G.F., 1985, Strontium, neodymium, and lead isotopic compositions of deep crustal xenoliths from the Snake River Plain evidence for Archean basement. Earth and Planetary Science Letters, v. 75, p. 354–368.

Leeman, W P., Oldow, J.S , and Hart, W K , 1992, Lithosphere-scale thrusting in the western U.S. Cordillera as constrained by Sr and Nd isotopic transitions in Neogene volcanic rocks: Geology, v 20, p. 63–66

Link, P.K., and Phoenix, E.C., 1996, Rocks Rails & Trails, 2nd Edition, Idaho Museum of Natural History, 194 p.

Luessen, M.J., 1987, Geology of Massacre Volcanic Complex, eastern Snake River Plain, Idaho. [M.S. thesis]: Pocatello, Idaho State University, 163 p.

Lum, C.C., Leeman, W.P., Foland, K.A., Kargel, J.A., and Fitton, J.G., 1989, Isotopic variations of continental basaltic lavas as indicators of mantle heterogeneity. examples from the western U.S. Cordillera. Journal of Geophysical Research, v. 94, p. 7871–7884.

Malde, H.E., 1991, Quaternary geology and structural history of the Snake River Plain, Idaho and Oregon; *in* Morrison, R.B., ed., Quaternary nonglacial geology; Conterminous U.S.. Boulder, Colorado, Geological Society of America, The Geology of North America, v. K-2, p. 251–281.

Manga, M., 1995, Waves of bubbles in basaltic magmas and lavas: Journal of Geophysical Research, vol. 101, No. B8, p. 17,457–17,465

McCurry, M., Bonnichsen, B , White, C., Godchaux, M , and Hughes, S , 1997, Bimodal basalt-rhyolite magmatism in the central and western Snake River Plain, Idaho and Oregon, this volume.

Menzies, M.A , Leeman, W.P., and Hawkesworth, C.J., 1983, Isotope geochemistry of Cenozoic volcanic rocks reveals mantle heterogeneity below western USA. Nature, v. 303, p. 205–209.

Morin, R.H., Barrash, W., Paillet, F.L., and Taylor, T.A., 1993, Geophysical logging studies in the Snake River Plain aquifer at the Idaho National Engineering Laboratory—wells 44, 45, and 46. U.S. Geological Survey Water-Resources Investigations Report 92-4184, 44 p.

Morin-Jansen, A , 1987, Study of the principle lineament and associated lineaments [M.S. thesis]. Pocatello, Idaho State University, 79 p.

Muller, O.H., and Pollard, D.D., 1977, The stress state near Spanish Peaks, Colorado, determination from a dike pattern: Pure and Applied Geophysics, v. 115, p. 69–86.

Noble, D.C., Rigot, W.L., and Bowman, H.R., 1979, Rare-earth-element content of some highly differentiated ash-flow tuffs and lavas; *in* Chapin, C E , and Elston, W.E , eds., Ash-Flow Tuffs, Geological Society of America Special Paper 170, p. 77–85.

Olsen, G L , 1996, Soil erosion results. Interdepartmental Communication #GLO-01-96, Lockheed-Martin Idaho Technologies Company, 5p.

Pierce, K.L., and Morgan, L.A., 1992, The track of the Yellowstone hotspot. Volcanism, faulting, and uplift; *in* Link, P.K., Kuntz, M.A., and Platt, L.P., eds., Regional geology of eastern Idaho and western Wyoming: Geological Society of America Memoir 179, p. 1–53.

Pierce, K.L., Fosberg, M.A., Scott, W.E., Lewis, G.C., and Coleman, S.M., 1982, Loess deposits of southeastern Idaho. age and correlation of the upper two loess units; *in* Bonnichsen, Bill, and Breckenridge, R.M., eds., Cenozoic Geology of Idaho, Idaho Bureau of Mines and Geology Bulletin 26, p. 717–725.

Pollard, D.D., Delaney, P.T., Duffield, W.A., Endo, E.T., and Okamura, A.T., 1983, Surface deformation in volcanic rift zones. Tectonophysics, v.94, p.541–584.

Prinz, M., 1970, Idaho rift system, Snake River Plain, Idaho: Geological Society of America Bulletin, v. 81, p. 941–947.

Rathburn, S L., 1991, Quaternary channel changes and paleoflooding along the Big Lost River, Idaho National Engineering Laboratory. Idaho National Engineering Laboratory Informal Report EGG-WM-9909, 33 p.

Rathburn, S.L., 1993, Pleistocene cataclysmic flooding along the Big Lost River, east central Idaho Geomorphology, v 8, p. 305–319.

Reed, M F, Bartholomay, R C., and Hughes, S.S., 1997, Geochemistry and stratigraphic correlation of basalt lavas beneath the Idaho Chemical Processing Plant, Idaho National Engineering Laboratory. Environmental Geology, v. 30, p. 108–118.

Reid, M.R., 1995, Processes of mantle enrichment and magmatic differentiation in the eastern Snake River Plain. Th isotope evidence. Earth and Planetary Science Letters, v. 131, p 239–254.

Richards, M.A., Duncan, R.A., and Courtillot, V.E., 1989, Flood basalts and hot spot tracks: Plume heads and tails: Science, v. 246, p. 103–107

Rodgers, D.W., Hackett, W.R., and Ore, H.T., 1990, Extension of the Yellowstone Plateau, eastern Snake River Plain, and Owyhee Plateau Geology, v. 18, 1138–1141.

Rubin, A.M , 1992, Dike-induced faulting and graben subsidence in volcanic rift zones· Journal of Geophysical Research, v. 97, no. B2, p. 1839–1858.

Rubin, A.M., and Pollard, D.D., 1987, Origins of blade-like dikes in volcanic rift zones: U.S. Geological Survey Professional Paper 1350, Chapter 53, p. 1449–1470.

Rubin, A.M., and Pollard, D.D., 1988, Dike-induced faulting in rift zones of Iceland and Afar: Geology, v.16, p 413–417.

Scott, W.E., 1982, Surficial geologic map of the eastern Snake River Plain and adjacent areas, Idaho and Wyoming: U S Geological Survey Miscellaneous Investigation Map I-1372, scale 1:250,000

Shaw, H.R., 1980, The fracture mechanism of magma transport from the mantle to the surface; *in* Hargraves, R.B , ed., Physics of Magmatic Processes. Princeton University Press, p.202–264.

Smith, R.B., and Sbar, N.L., 1974, Contemporary tectonics and seismicity of the western United States with emphasis on the Intermountain Seismic Belt. Geological Society of America Bulletin, v 85, p. 1205–1218.

Smith, R.B , and Braile, L.W., 1994, The Yellowstone hotspot: Journal of Volcanology and Geothermal Research, v. 61, p. 121–187.

Smith, R.P, Hackett, W R., and Rodgers, D.W., 1989, Geological aspects of seismic hazards assessments at the INEL, southeastern Idaho: Proceedings of the Second DOE Natural Hazards Mitigation Conference, Knoxville, Tennessee, p 282–289.

Smith, R.P., Jackson, S.M., and Hackett, W.R., 1996, Paleoseismology and seismic hazards evaluations in extensional volcanic terrains· Journal of Geophysical Research, v. 101, no. B3, p. 6277–6292.

Spear, D.B., 1979, The geology and volcanic history of the Big Southern Butte-East Butte area, eastern Snake River Plain, Idaho. State University of New York at Buffalo Ph.D. Dissertation, 136 p.

Spear, D.B., and King, J.S., 1982, The geology of Big Southern Butte, Idaho; *in* Bonnichsen, Bill, and Breckenridge, R.M., eds., Cenozoic Geology of Idaho, Idaho Bureau of Mines and Geology Bulletin 26, p 395–403.

Stearns, H.T., Crandall, L., and Steward, W.G., 1938, Geology and ground-water resources of the Snake River Plain in Southeastern Idaho: U.S. Geological Survey Water Supply Paper 774, 268 p.

Stout, M.Z., and Nicholls, J., 1977, Mineralogy and petrology of Quaternary lava from the Snake River Plain, Idaho. Canadian Journal of Earth Sciences, v. 14, p. 2140–2156.

Stout, M.Z., Nicholls, J., and Kuntz, M.A., 1994, Petrological and mineralogical variations in 2500–2000 yr B.P lava flows, Craters of the Moon lava field, Idaho. Journal of Petrology, v. 35, p. 1682–1715.

Suppe, J., 1985, Principles of structural geology. Prentice-Hall, Englewood Cliffs, NJ, 537 p.

Thompson, R.N., 1972a, The 1-atmosphere melting patterns of some basaltic series. American Journal of Science, v. 272, p 901–932.

Thompson, R.N., 1972b, Melting behavior of two Snake River lavas at pressures up to 35 kb. Carnegie Institution of Washington, Geophysical Laboratory Yearbook, v. 71, p 877–905.

Thompson, R.N., 1975, Primary basalts and magma genesis-II Snake River Plain, Idaho. Contributions to Mineralogy and Petrology, v. 52, p. 213–232

Trimble, D.E., and Carr, W.J., 1976, Geology of the Rockland and Arbon Quadrangles, Power County, Idaho. U.S. Geological Survey Bulletin 1399, 115 p.

Welhan, J., Funderberg, T, Smith, R.P., and Wylie, A., 1997, Stochastic modeling of hydraulic conductivity in the Snake River Plain Aquifer: 1. Geologic constraints and conceptual approach; *in* Sharma, S., and Hardcastle, J.H, eds., Proceedings of the 32nd Symposium on Engineering Geology and Geotechnical Engineering, p 75–91

Wetmore, P.H., Hughes, S S, Anderson, S.R., 1997, Model morphologies of subsurface Quaternary basalts as evidence for a decrease in the magnitude of basaltic magmatism at the Idaho National Engineering and Environmental Laboratory, Idaho; *in* Sharma, S, and Hardcastle, J H, eds., Proceedings of the 32nd Symposium on Engineering Geology and Geotechnical Engineering, p. 45–58

Wohletz, K.H., and Sheridan, M.F., 1983, Hydrovolcanic Explosions II Evolution of basaltic tuff rings and tuff cones American Journal of Science, v 283, p. 385–413.

Womer, M.B., 1977, The origin of Split Butte, a maar type crater of the south-central Snake River Plain, Idaho; *in* Greeley, R, and King, J.S., eds., Volcanism of the eastern Snake River Plain, Idaho A Comparative planetary guidebook Washington, D C, National Aeronautics and Space Administration, p. 190–202

Womer, M B, Greeley, R., and King, J S., 1982, Phreatic eruptions of the eastern Snake River Plain of Idaho, *in* Bonnichsen, Bill, and Breckenridge, R.M., eds., Cenozoic Geology of Idaho. Idaho Bureau of Mines and Geology Bulletin 26, p 453–464